Faculdade de Engenharia da Universidade do Porto

Wireless Communication over NFC with a Constrained Resource Device

André Filipe Mendes Raposo

Work carried out in the framework of the curricular unit
Dissertação
at the DRAMCO research group, KaHoSint-Lieven Hogeschool Gent
Mestrado Integrado em Engenharia Electrotécnica e de Computadores
Major Telecomunicações

FEUP Supervisor: Prof. Dr. José Machado Silva
DraMCo Supervisor: Ing. Tom Hamelinckx

31.07.2010

A Dissertação intitulada

"WIRELESS COMMUNICATION OVER NFC WITH A RESOURCE CONSTRAINED DEVICE"

foi aprovada em provas realizadas em 19/Julho/2010

o júri

Presidente Professor Doutor João Paulo de Castro Canas Ferreira
Professor Auxiliar do Departamento de Engenharia Electrotécnica e de Computadores da Faculdade de Engenharia da Universidade do Porto

Professor Doutor Luís Alexandre Machado Rocha
Professor Convidado Equiparado a Professor Associado da Escola de Engenharia da Universidade do Minho

Professor Doutor José Alberto Peixoto Machado da Silva
Professor Associado do Departamento de Engenharia Electrotécnica e de Computadores da Faculdade de Engenharia da Universidade do Porto

O autor declara que a presente dissertação (ou relatório de projecto) é da sua exclusiva autoria e foi escrita sem qualquer apoio externo não explicitamente autorizado. Os resultados, ideias, parágrafos, ou outros extractos tomados de ou inspirados em trabalhos de outros autores, e demais referências bibliográficas usadas, são correctamente citados.

Autor - André Filipe Mendes Raposo

Faculdade de Engenharia da Universidade do Porto

Resumo

Este estudo foi realizado no âmbito de um projecto desenvolvido na Bélgica no centro de investigação DraMCO associado à universidade KaHo Sint-Lieven no âmbito do programa Erasmus. O projecto tem como objectivo implementar um sistema electrónico integrado numa bracelete de pulso. Este dispositivo deve ser capaz de comunicar usando vários protocolos de comunicação como *Bluetooh* ou *Near Field Communication*.

Para alimentar o dispositivo é usada uma tecnologia recente: Energy harvesting. Mais concretamente, é usado um gerador piezoeléctrico que converte energia mecânica em energia eléctrica. Mas para uma melhor eficácia o gerador precisa de um sistema de gestão de energia e para tal, é usado um circuito integrado recente da *Linear Technology*, o LTC3588-1. Assim, aplicar este dispositivo de gestão de energia em conjunto com uma unidade de armazenamento de energia constituída por um supercondensador, conduziu a resultados muito positivos. O sistema conseguiu alimentar o dispositivo durante algumas horas mesmo sem a presença de uma fonte de vibração. A título de conclusão, a utilização de tecnologias de conversão de energia ambiente em energia eléctrica (Energy Harvest) é uma alternativa a considerar quando se pretende alimentar dispositivos portáteis e de baixo consumo.

Abstract

This study was carried out in the framework of a high level project developed in Belgium on DraMCo research group associated with KaHo Sint-Lieven University. The project aims the implementation of an electronic system integrated in a wrist strap capable of interact with several communication technologies such as: *Bluetooth and Near Field Communication (NFC)*. In the present project a power system is studied as well as the NFC communication protocol.

To power the device a recent energy technology is approached: Energy harvesting. More specifically, a piezoelectric generator is used to convert the vibration energy into electric. However, the piezoelectric cannot power the device only by its own because it needs a system to manage the energy that produces. Therefore, a recent energy management chip of Linear Technology is used, the LTC3588-1. Using this chip together with a big storage unit constituted by a supercapacitor, lead to very positive results. The system could power the device for a few hours even without the presence of a vibration source. Energy harvest is an alternative to consider when feeding low power portable devices is desired.

Acknowledgements

I would like to thanks to my supervisors for all their advices and guidance during this master thesis. A special word also to the eternal and unconditional support provided by my parents.

Contents

List of Figures

List of Tables

Acronyms and Symbols

CMOS	Complementary Metal-Oxide Semiconductor
ECMA	European association for standardizing information and communication systems
FEUP	Faculdade de Engenharia da Universidade do Porto
ISO/IEC	International Organization for Standardization/International Electrotechnical Commission
MEMS	Micro-Electro-Mechanical Systems
NFC	Near Field Communication
PCB	Printed Circuit Board
RFID	Radio Frequency Identification
RF	Radio Frequency

Chapter 1

Introduction

1.1 - Introduction

The work presented herein was conducted under the scope of the *Dissertação* curricular unit of the Master program in Electrotechnical and Computer Engineering of the *Faculdade de Engenharia da Universidade do Porto* (FEUP). It was developed during an internship under the ERASMUS program at the DraMCo research group of the electronic department of KaHoSint-Lieven Hogeschool Gent. This recently created research group has as main research topics the reduction of circuit's power consumption together with the development of secure applications environments for wireless systems such as *RFID*. The present research's purpose lies in between these two study fields and is part of a project that aims to build a low power portable wireless communication interface.

Designed to be used as a wristwatch, this device must be able to communicate over several communication protocols such as *Bluetooth* or *NFC* (Near Field Communication) as well as to consume the lowest energy possible. In addition, the watch user targets are swimmers or general sportsmen that wish to use the device's memory to store data related to their performance historic in order to evaluate their evolution or only to store personal data such as identification, health condition or blood type.

1.2 - Objectives

This work is focused on one of the several development stages of this wireless interface communication device, the power consumption. Since the device is portable the need for an autonomous and efficient power system is mandatory. Therefore, the main objective is to project and implement an independent system capable of feeding one of the device's communication interfaces. In order to be aware of some of the latest power technologies

available the research starting point is the study of a recent power technology known as *Energy Harvesting*. From this point other options will also be analysed in order to find the optimal final powering system. In the end and as a final product, a printed circuit board (PCB) was designed and assembled. In addition to the powering system, this board will uses a low-power microcontroller whose software has been optimized by software to ensure minimum operational power consumption. Moreover, the study will lean over the NFC communication technology. Although no communication procedures are implemented and tested, some studies are carried out in order to know its operation principles and naturally its necessities regarding energy needs.

1.3 - Document Structure

Further to this introduction, this document contains five chapters more. In the following two chapters is presented all the research done about both Energy Harvest and Near Field Communication technologies. In chapter two an overview about several energy conversion methods is carried out as well as an analysis about the procedure followed to obtain and manage the energy used in the present research. In chapter three all the details inherent to the NFC communication protocol and operation procedures are described.

The next two chapters are related to the practical work performed during the research. In chapter four the tests made to the first power system scheme are described as well as its results. After this, the results analysis and the respective conclusions are presented. In chapter five the final system is described as well as the tests performed on it. Next, the performance and the final results are discussed and some conclusions are drawn.

The final chapter is nothing more than a conclusion of the entire work performed: the final prototype, future improvements and even personal achievements.

Chapter 2

Energy Harvesting

2.1 - Introduction

Energy Harvesting, also known as energy scavenging, is a process where available and unused environmental energy is captured and stored as useable electrical energy so it can also be classified as *free energy*. Usually, this designation is applied when speaking of low grade ambient sources such as environmental vibrations, human power, thermal sources, solar, wind and electromagnetic energy. Despite free and abundant these surrounding sources of energy present a property that limits its extent of use, they are only available in very small packets which makes them very hard to capture. However, due to its enormous potential, the research amount in this field has increased and positive results were achieved with the development of new products and technologies that can overcome this limitation and therefore use free energy.

The continuous transistor's size high shrinking rate foreseen in the *Moore's law* along with its supply voltage reduction, resulted on an overall decrease in power consumption overCMOS circuits. This evolution led to the creation of diverse high efficiency and low power technologies. These new products allow capturing, store and converting the small energy packets into useful output by using management systems that are able to store energy for long periods of time. Due to the unpredictability and variability nature of the surrounding energy, these circuits also tolerate a wide range of voltage, current and waveform inputs.

The present chapter introduces the environmental energies studied along the project and the principles governing its extraction technology – the *Transducer*. In addition, an overview about general energy management systems is exposed along with the system tested during this work.

2.2 - MEMS

In spite of the increasing miniaturization of mobile electronics such as wireless sensors, and of the reduction of their power consumption, portable systems still demand the creation of alternative power sources because the traditional ones such as batteries are limiting this progress by having a large size, weight and cost. Some designers claim that first the battery or power source must be specified and only after design the mobile device's electronic around it [21].

MEMS technologies play an important role in this progress enabling the creation of smaller, lighter and with infinite life time powering systems. It is due to this technology development that transducer's systems power consumption was reduced from the order of W to mW level [8] which led to the availability of a higher efficiency and effectiveness energy capture and enabled a new research area: supply power to microsystems threw from environmental energy. On the other hand a MEMS fabrication technology ensures the advantage of mass production which can be useful in the future in case energy harvesting technology is commercialized.

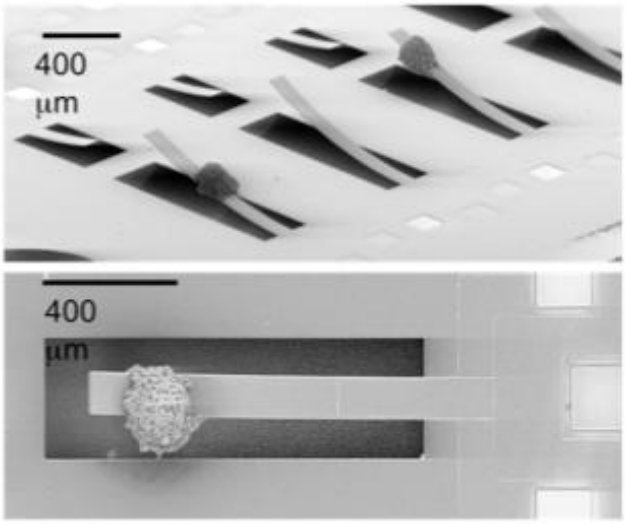

Figure 2.1 - MEMS structure.

2.3 - Mechanical Energy

Mechanical energy is the energy resulting from motion, displacement or vibration. The latter is particularly attractive due to its abundance. Mechanical vibration energy has been intensively studied because it exists everywhere in our environment spread along different surroundings: human body, vehicles, structures, industrial and the environment itself [27]. In order to convert it to electricity three different transducers can be used: electrostatic,

electromagnetic and piezoelectric. An electrostatic transducer consists of a fixed electrode and a moveable electrode, charged electrostatically with the opposite polarity. The motion of the movable electrode changes the capacitance between the electrodes and thereby makes the applied voltage change in proportion to the amplitude of the electrode's motion that causes a voltage change across the capacitor resulting in a current flow in an external circuit. Due to its converting mechanism this transducer is also known as condenser transducer. Another converting technology is the electromagnetic transducer where the relative motion of a magnetic mass with respect to a coil causes a change in the magnetic flux. The magnetic variation produced generates an AC voltage across the coil. Compared with the two former transducers, piezoelectric transducers show advantages such as simple configuration, higher conversion efficiency, and more precise control of the mechanical response [16].

2.3.1 - Piezoelectricity

In the year of 1880 an unusual characteristic in certain crystalline minerals was discovered. When mechanical stress was applied to these materials, an electrical charge was generated. This charge was proportional to the applied force. This property was named *Piezoelectricity*, from the Greek word *piezein* that means pressure. The studies proceeded about this property and soon determined that, conversely, when such crystals are applied to an electric field they change their shape according to the polarity of the field. However, piezoelectricity remained nothing more than a laboratory curiosity for a few years. Only in during World War I, this material property was used to create a device, an ultrasonic submarine detector – the sonar. The success of this project led to an intense development interest in devices using this technology and research increase in this area. Nowadays, these piezoelectric devices can be found in several different fields. For example: the piezoelectric igniter, that generates a spark by compressing a piezoelectric material disc, used to ignite small engine ignition systems such as gas-grill, devices like loudspeakers also use piezoelectric material to convert voltage in vibration in order to produce sound.

2.3.1.1 - Dipole Moment and Weiss Domains

The *Dipole Moment* is a vectorial measure of the separation between positive and negative electrical charges in a charges system or in other words it measures the system's overall polarity. For a pair of opposite charges but with the same magnitude *q*, the dipole is defined as the product of the charges magnitude and the distance between them and its direction is defined towards the positive charge. The electric dipole moment *p* is:

$$\vec{p} = q\vec{d}\ (D)\ , \tag{2.1}$$

where *d* is the displacement vector point from the negative charge to the positive charge and *q* is the charge magnitude as shown in Fig.2.2.

When referring to molecules, their dipole moment is the vector sum of the dipole moments of the different bonds,

$$\vec{p} = \sum_{i=1}^{N} q_i \vec{d}_i \ (D), \tag{2.2}$$

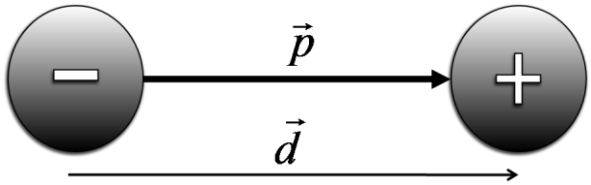

Figure 2.2 - Dipole moment vectors.

Still, the dipole depends not only on the individual dipole moments of each connection but also on the spatial arrangement of the various bonds in the molecule. The sum of dipole moments (Eq.2.2) of each molecule bond helps to distinguish between polar and non-polar molecules. Non-polar molecules have a zero dipole moment because the dipoles cancel each other unlike polar molecules that have some value of dipole moment. For example the Carbon dioxide (CO_2) is a non-polar molecule but on the other hand the water molecule (H_2O) is a polar one.

Carbon dioxide is a linear molecule in which the two bonds present the same dipole moment value but they are oriented in opposite directions at an angle of 180^0 and due to this linear geometry the dipole moment of one carbon oxygen bond cancels that of another. Therefore, the resultant dipole moment of the molecule is zero and it is classified as a non-polar molecule (Fig.2.3).

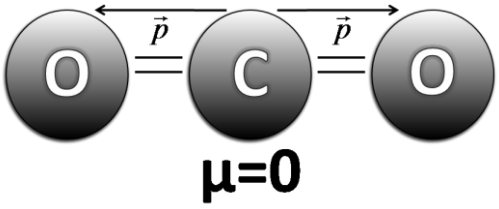

Figure 2.3 - CO_2 molecule dipole moment.

Whereas, the water has two oxygen hydrogen bonds but oriented asymmetrically at an angle of 105^0, this way the resultant of dipole moments is not zero making a water molecule polar.

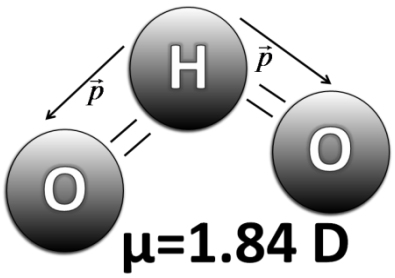

Figure 2.4 - H_2O molecule dipole moment.

Weiss domains are nothing more than areas in a crystal structure organized by groups of dipoles with parallel orientation.

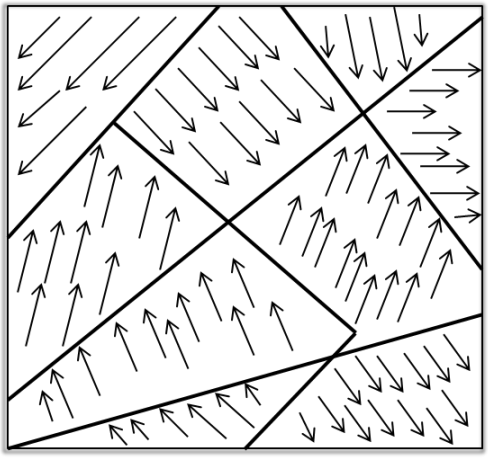

Figure 2.5 - Weiss domains.

These two concepts are crucial to understand the way how the piezoelectric effect occurs.

2.3.1.2 - Materials

Quartz is a well known single crystal material with piezoelectric capabilities, it is used in the majority of wrist watches to generate a fixed clock frequency. Besides quartz other vulgar materials such as Topaz and Bone have piezoelectric properties. But among all the materials, the most important group is the man-made piezoelectric ceramics such as Barium Titanate. This ceramic was the first to be discovered and was used for a very long time due to its ease of production and high coupling factor when comparing to the natural crystals. However, this material had a serious weakness: excessive aging due to temperature because of the materials low *Curie point*. One method to overcome this limitation was to add other materials such as lead (Pb) or Calcium (Ca) [15]. Especially, the addition of Pb had a positive effect in increasing the Curie point temperature, leading to the discovering of PZT ceramics,

which had much better temperature and aging characteristics than Barium Titanate. This type of ceramics can be hundreds of times more sensitive to electrical or mechanical input than natural materials and can be fashioned into components of almost any shape and size. They are physically strong, chemically inert and immune to humidity or other atmospheric influences and can also be produced relatively inexpensively. These characteristics make the PZT the most common material used to produce piezoelectric elements.

The PZT ceramic is usually a solid solution of Lead Titane ($PbTiO_{3)}$) or Lead Zirconate ($PbZrO_3$) and despite being the most common type of ceramics other ones can be produced to serve specific purposes. A traditional piezoelectric ceramic has a *perovskite* crystal structure, a tetragonal structure arranged by a general chemical formula ABX_3 in which 'A' denotes a large divalent metal ion such as lead - Pb- or barium - Ba- and 'B' denotes a small tetravalent metal ion such as zirconium -Zr - or titanium - Ti. Both 'A' and 'B' are cations bonded by 'X', an anion such as an oxygen element – O.

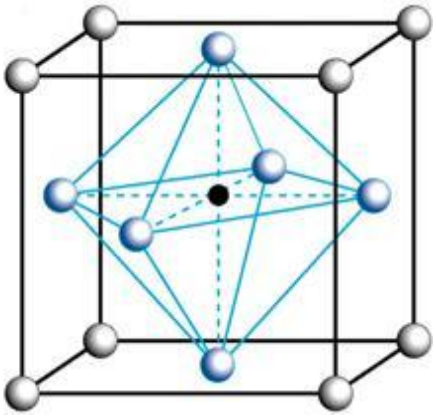

Figure 2.6 - Perovskite structure.

The perovskite structure materials play an important role in piezoceramics as variations of ionic size and small displacements of atoms that lead to a distortion of the structure and a reduction of symmetry have profound effects on their physical properties. These structures also have a special property related to the temperature. Above the critical temperature, the Curie point, each perovskite crystal has a simple cubic symmetry with no dipole moment, but if the material is below the Curie point a displacement of the central cation occurs, Fig.2.7. Changing the crystal structure induces a net dipole moment or a polarization that can be modified by applying an electric field. This is the phenomenon that provides piezoelectric properties to PZT ceramics piezoelectric properties. Only with a temperature below the Curie point the material behaves like piezoelectric material, while above it the material loses its polarization and its piezoelectric characteristics.

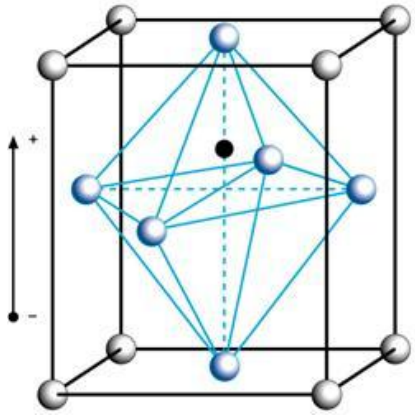

Figure 2.7 - Perovskite structure with a dipole moment.

2.3.1.3 - Fabrication Process

After a first phase where the fine metal powders are heated and mixed with an organic binder they are finally molded in the desired shape. Then the elements are cooled and the electrodes are applied to the appropriate surfaces. At this stage we can say that the piezoelectric material is in its raw condition, the material presents randomly oriented *Weiss domains* and due to this orientation disorder the ceramic element has no overall polarization and therefore will not exhibit piezoelectric effect.

Afterwards, the *Poling* process is carried out. A process where a strong electric field is applied across with the objective is to align the dipoles with the electric field to a point that even after the field is removed the dipoles or at least most of them remain locked in that configuration. This way the ceramic material became piezoelectric with permanent polarization and deformation.

Figure 2.8 - Piezoelectric devices with different shapes.

2.3.1.4 - The piezoelectric effect

After the piezoelectric unit fabrication is complete and tested it is ready to be used as a transducer. These devices can operate in two different ways: as motors or as generators. As motors the piezoelectric transducer converts electrical energy into mechanical energy by the other side the generators transform a mechanical stress into voltage.

After poling the material dipoles are nearly aligned with the previous applied electric field. However, when a voltage is applied, this alignment increase which leads to a change in the material dimension or a mechanical deformation, as shown in Fig.2.9. If a voltage of the same polarity as the poling voltage is applied to a ceramic element, in the direction of the poling voltage, the element will lengthen. If a voltage of polarity opposite to that of the poling voltage is applied, the element will become shorter, Fig.2.10. Also if an alternating voltage is applied, the element will lengthen and shorten cyclically, at the frequency of the applied voltage.

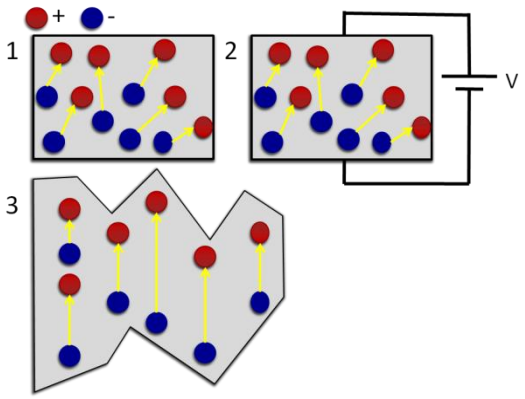

Figure 2.9 – Piezoelectric effect voltage applied. (1) Charges near aligned. (2) Voltage applied. (3) Dimension change.

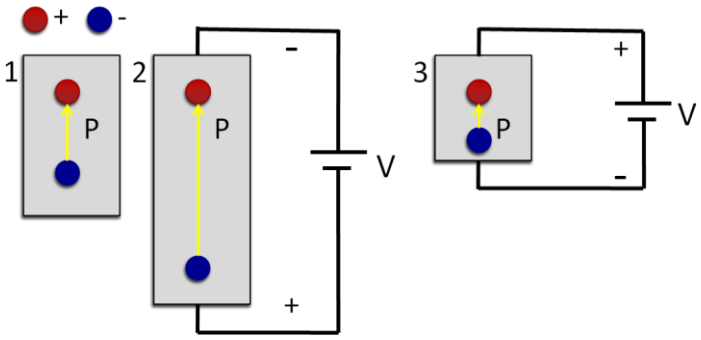

Figure 2.10 - Piezoelectric effect voltage applied. (1) Material after poling. (2) Material lengthens. (3) Material shortens.

Although not perfect aligned, the dipole effects of the piezoelectric element are symmetric and cancel each other. Therefore the dipole moment is zero, which means that the overall polarization is null. But when a mechanical force is applied some elastic deformation is induced and the symmetry is broken which forces the charges out of balance.

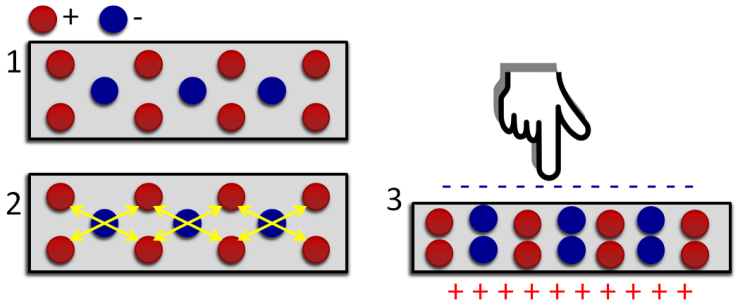

Figure 2.11 - Piezoelectric effect deformation. (1) Charges balanced. (2) Dipole moments cancel one another out. (3) Charges unbalanced with mechanical stress.

This way, the dipoles will no longer cancel each other and a polarization will occur, charges will appear in the crystal surface resulting in a voltage difference between the surfaces where the electrodes are placed. This induced voltage can be used to generate electrical energy. Compression along the direction of polarization, or tension perpendicular to the direction of polarization, generates voltage of the same polarity as the poling voltage. Tension along the direction of polarization, or compression perpendicular to the direction of polarization, generates a voltage with polarity opposite that of the poling voltage.

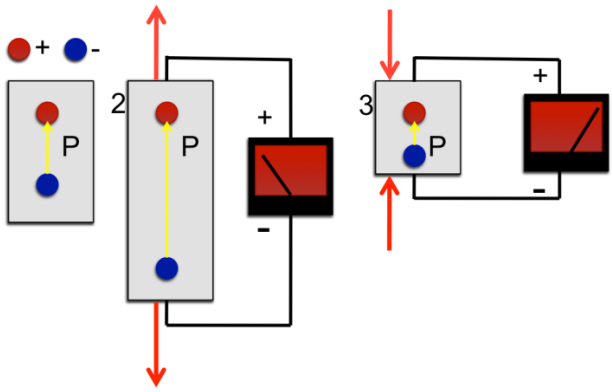

Figure 2.12 - Piezoelectric effect deformation. (1) Material after poling. (2) Polarity≠Poling. (3) Polarity=Poling.

2.3.1.5 - Piezoelectric Transducer

The piezoelectric *transducer* is a device that converts mechanical energy in electrical energy as well as electrical energy in mechanic deformation taking advantage of the

piezoelectric effect. They are commonly used in applications such as pressure, strain and acceleration sensors since it converts these inputs into an electrical measurable signal and also in devices such as *earphones* where an alternating current is applied to a piezoelectric crystal resulting in a continuous mechanical deformation that produces sound.

2.3.1.6 - Piezoelectric Vibration Induced Power Generator

Although alternate structures are being developed in order to increase the device efficiency [10], the shape commonly used for a transducer of this kind is a cantilever beam. This design, shown in Fig.2.13, can produce low resonant frequencies and relatively high displacement for a given mechanical force input or in other words: is a high sensitive vibration structure. The piezoelectric vibration-induced power generating principle can be described with an electrical and mechanical equivalent system based upon a conventional second-order system. Let's consider the model in the Fig.2.13 that shows a general example of such a system, the cantilever beam and it equivalent mechanic model. The model is based on a seismic mass, *m*, and the equivalent spring constant, *k*. The energy losses within the system due to the transfer of mechanical energy to the electrical load and parasitic effects are represented by the damping coefficient *b* [17], and all the elements are located within an inertial frame.

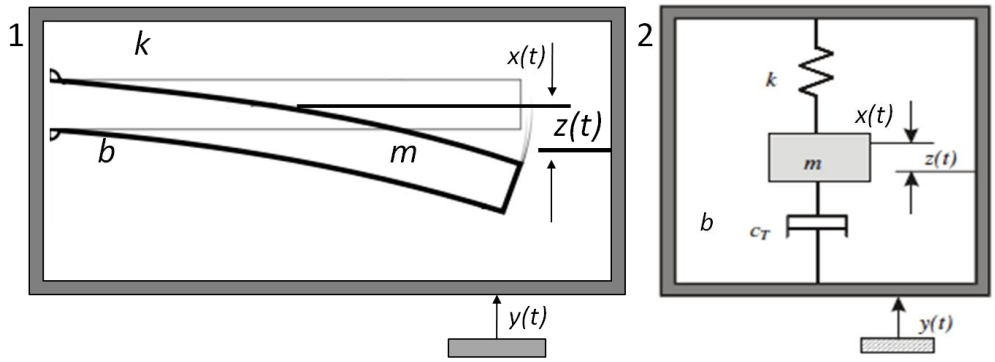

Figure 2.13 - (1) Cantilever beam. (2) It mechanic model.

The displacement applied to it, *y(t)*, the system input, causes a displacement, *x(t)*, which is the system output. This results in a net displacement, *z(t)*= x(t)-y(t) that is the relative displacement of the mass. The system can be modeled as:

$$m\left[\ddot{x}(t)-\ddot{y}(t)\right]+b\left[\dot{x}(t)-\dot{y}(t)\right]+k\left[x(t)-y(t)\right]=-m\ddot{y}(t)\,, \tag{2.1}$$

or,

$$m\ddot{z}(t)+b\dot{z}(t)+kz(t)=-m\ddot{y}(t)\,, \tag{2.2}$$

Taking the Laplace transformation of the above equation, it becomes,

$$-V_{in}(s) = I(s)\left[sL + \frac{1}{Cs} + R \right], \tag{2.3}$$

By analogy to an electric system, the equivalent circuit is,

$$-ms^2Y(s) = sZ(s)\left[ms + \frac{k}{s} + b \right], \tag{2.4}$$

Where $V_{in}(s)$ is the voltage source and is analogous to the input force. And $I(s)$, the loop current that is analogous to the relative velocity of the mass. The analogy between Eq. (2.3) and Eq. (2.4) is,

$$\begin{aligned} &V_{in}(s) = ms^2Y(s), \\ &I(s) = sZ(s), \\ &C = \frac{1}{k}, \\ &R = b, \\ &L = m. \end{aligned} \tag{2.5}$$

So, Eq. (2.4) can be rewritten as,

$$-V_{in}(s) = \frac{1}{C}\frac{I(s)}{s} + I(s)\left[sL + R \right] \tag{2.6}$$

This equation describes the electrical analogue of a mechanical vibrating mass system and is represented in Fig.2.14.

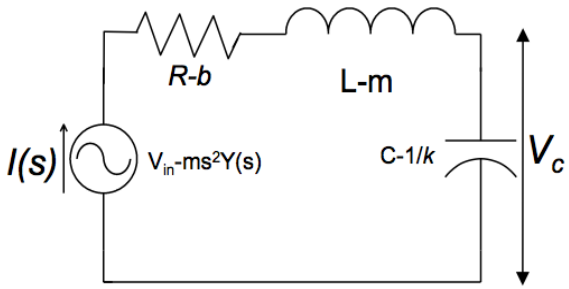

Figure 2.14 - Cantilever electrical equivalent.

When a piezoelectric film is attached to the beam top and bottom surfaces as shown in Fig.2.15, the beam bending produces a tension in the top layer and compresses the bottom. This will develop a voltage across each of the layers and induces a potential difference V_x between both. This way the simple cantilever beam system becomes a vibration-induced power generator since the mechanical energy stored in the spring is converted to electrical

energy through the piezoelectric element that acts as a transducer making the conversion between both energies.

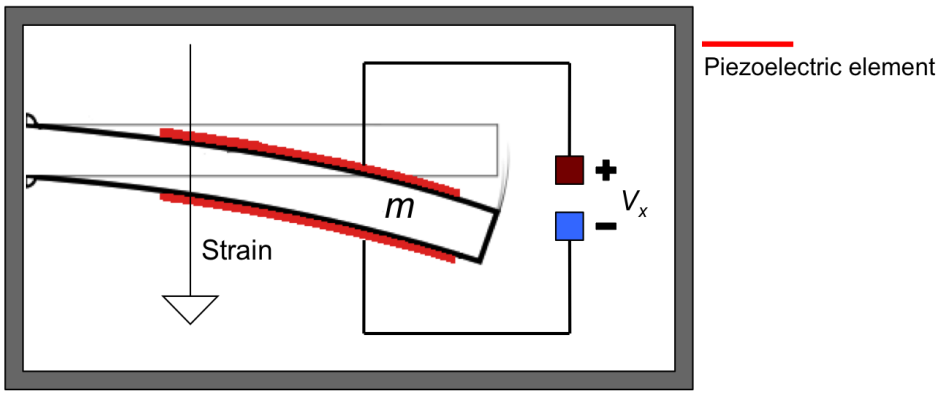

Figure 2.15 - Piezoelectric transducer.

Most of power generators instead of using one cantilever beam use two, one on top of the other resulting on a two layer cantilever bender, or a *bimorph*. Usually a neutral central layer, typically metal, is placed between both layers. This central elastic layer adds robustness, as the ceramic is very brittle, and also can improve the overall electromechanical coupling. The complete equivalent circuit of the power generator is presented Fig.2.16 where C_p and R_g>>0 are equivalent capacitance and the loss of the piezoelectric element, respectively. The induced voltage can be regarded as the result of the C_p being charged by V_c.

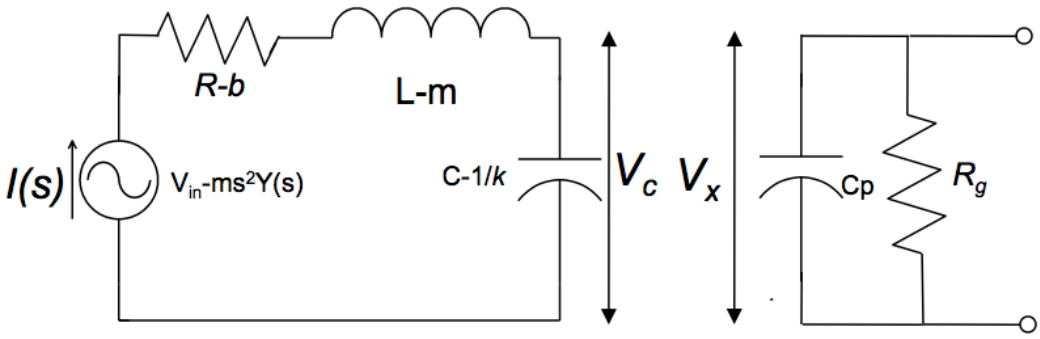

Figure 2.16 - Power generator electric equivalent.

Assume the energy conversion rate between the mechanical energy and the electrical energy is related by the transducer electromechanical coupling factor k_e. This factor is an indicator of the effectiveness which a piezoelectric material converts mechanical energy into electric energy or electrical energy in mechanic energy. A high coupling factor is desirable for efficient energy conversion because it reflects the ratio of the mechanical energy supplied by the beam and the useable energy delivered by the piezoelectric. This factor in a conceptual way can been seen as,

$$k_e = \sqrt{\frac{electrical\ energy\ stored}{mechanical\ energy\ supplied}}, \tag{2.7}$$

In a scalar formula this coefficient is given by a quotient between the electric energy and the mechanic energy [12],

$$k_e = \frac{\frac{1}{2}C_p V_x^{\,2}}{\frac{1}{2}CV_e^{\,2}}, \tag{2.8}$$

The maximum instantaneous energy induced by the piezoelectric element can be describe by,

$$E_c(s) = \frac{1}{2}C_p V_x^2 = \frac{1}{2}K_e C V_e^2 = \frac{1}{2}k_e C\left(\frac{I(s)}{Cs}\right)^2 = \frac{1}{2}k_e k\frac{m^2Y^2(s)s^4}{\left[ms^2+bs+k\right]^2}, \tag{2.9}$$

When a sinusoidal signal $y(t)=Y_0.cos(\omega t)$ is applied Eq.(2.9) can be rewritten as,

$$\left|E_c(\omega)\right| = \frac{kk_e m^2Y^2(\omega)}{2}\frac{\omega^4}{\left[k-m\omega\right]^2+\left[\omega b\right]^2} = \frac{k_e m^2Y^2(\omega)}{2k}\frac{\omega^4}{\left[1-\left(\frac{\omega}{\omega_n}\right)^2\right]^2+\left[\frac{2\xi}{m}\frac{\omega}{\omega_n}\right]^2}, \tag{2.10}$$

where,

$$\begin{aligned}\xi &= \frac{b}{2\omega_n}\\ w_n &= \sqrt{\frac{k}{m}} = \frac{d}{2l^2}\sqrt{\frac{E}{\rho}}\end{aligned}, \tag{2.11}$$

The natural resonance frequency ω_n indicates that depends only of the beam's thickness *d* and length *l* of the beam [12]. If the applied excitation frequency equals the resonance frequency (w_n) of the system, the beam displacement is maximum and the transducer converts the maximum instantaneous energy, and the maximum output power density can be obtained,

$$E_{c\max} = \left|E_c(\omega_n)\right| = \frac{k_e m^2 Y_o^2}{2k}\frac{m^2\omega_n^2}{(2\zeta)^2} = \frac{k_e m^4 Y_o^2 \omega_n^4}{8k\xi^2}, \tag{2.12}$$

Looking at equation 2.12 it is found that the maximum converted electrical energy is proportional to the coupling factor k_e, the beam mass *m*, the resonance frequency of the mechanical system, and the displacement induced by the external force, as well as that is inversely proportional to the equivalent spring constant k and the damping factorζ.

Using this approach it is possible to estimate an energy output value however, it is also useful to know how efficiently the energy is converted. The presented approach relates two

parameters: the coupling coefficient k_e and the quality factor Q. As referred the coupling coefficient influences the power output. As some studies show [10], when increasing coupling, power increases quickly to a point, beyond which, the increase is almost null, Fig.2.17. Nevertheless, because the coupling is usually below this value, especially for micro fabricated devices improving the coupling coefficient is an important research area.

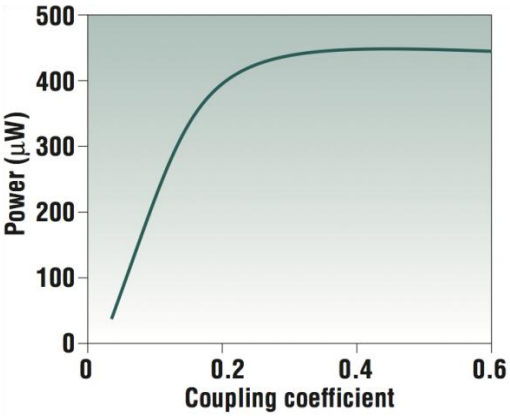

Figure 2.17 - Power vs. coupling coefficient [10].

The quality factor is in general a dimensionless parameter that describes resonator's bandwidth relative to its center frequency or resonance frequency. A high Q factor system resonates with great amplitudes at its natural frequency and has a low energy loss, which is desirable for an energy converter [16]. However its amplitude also decreases dramatically in the other frequencies resulting on a low bandwidth system. On the other hand systems with low Q resonate with higher amplitude at all frequencies but at its natural frequency the amplitude decreases in comparison to the high Q case. In addition, the quality factor is related to the damping factor, ζ by,

$$Q = \frac{1}{2\zeta}, \quad \Delta f = 2\zeta . f_n \qquad (2.13)$$

This means that the quality factor and consequently the damping factor are closely related to the system bandwidth range as shown on Fig.2.18.

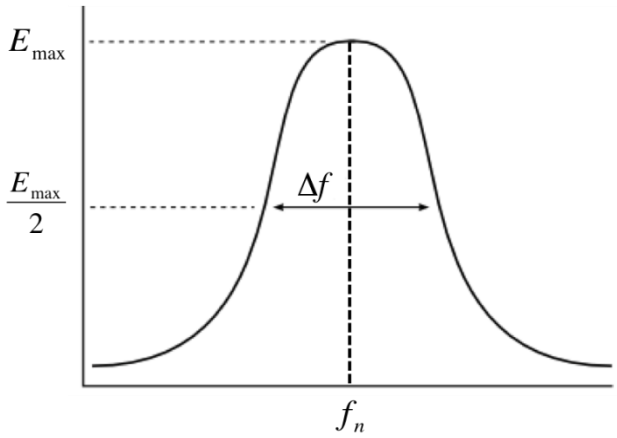

Figure 2.18 - Quality factor.

Finally the energy conversion efficiency of a piezoelectric element at its resonant frequency is given by [9],

$$\eta = \frac{\frac{k_e^{\,2}}{2(1-k_e^{\,2})}}{\frac{1}{Q}+\frac{k_e^{\,2}}{2(1-k_e^{\,2})}}, \tag{2.14}$$

The previous equation suggests that the efficiency is improved by increasing k_e and Q. Improving the coupling factor will always have positive repercussions in the power output since it raises the amount of energy converted and consequently the efficiency. Raising the Q factor can enhance the device efficiency on its resonant frequency but in certain vibration environments it may affect the device energy absorption since small deviations of the vibration frequency from the device's resonant frequency will induce significant reduction of the output power [16]. Therefore, a lower Q factor is sometimes preferred even with an overall efficiency loss.

Concluding, the parameters that most influence the efficiency of a piezoelectric vibration-induced power generator are the Q factor, the coupling coefficient k_e and resonant frequency w_n. By carefully selecting them, it is feasible to design a high efficiency piezoelectric power generator as they provide a useful guideline when choosing materials and designing generators. These parameters shall be selected according to the induced vibration frequency and the system's mechanical natural in order to match the desired power output.

2.3.1.7 - Wideband

As referred, vibration-based energy devices generate the maximum power when their resonance frequencies match the driving frequencies. In fact, power output drops off

dramatically as w_n deviates from w [10], this fact makes the resonant frequency of a vibration energy harvesting device one of the most important design parameters.

Naturally these generators are only efficient at the resonance frequency of the mechanical structure therefore they possess a low bandwidth vibration sensibility. Thus, when projecting a Piezoelectric Vibration Induced Power Generator the value of this parameter is crucial for the device performance.

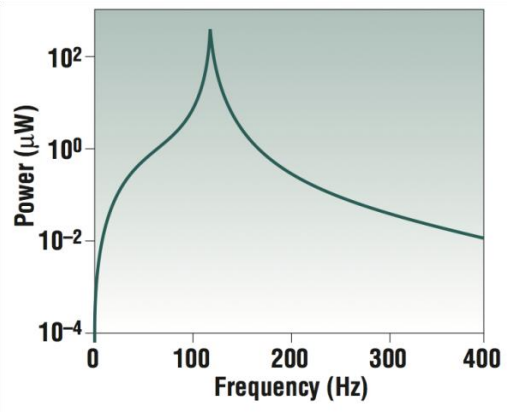

Figure 2.19 - Power vs. frequency [10].

When the vibration source frequency is regular and unique over the time it is possible to create a model and construct a device with certain efficiency, selecting the appropriate parameters in order to match the known environmental resonance frequency. However, once the device is fabricated and installed for use, it is a matter of chance for the frequency of ambient vibrations to match the optimum operating frequency. Due to fabrication accuracy is really hard to match the resonance frequency of the device to that of the environmental. Another limitation is the device behaviour in an irregular and multiple vibration frequency scenarios. The power generator only absorbs vibration energy with a frequency corresponding to its natural one, this way, would only absorb part of the vibration energy resulting on a waste of energy considering the energy in the other frequencies. Under these circumstances there is high energetic inefficiency as well as a non-optimized power output since most of the energy is being lost instead of being transformed in useable energy. Given this, it would be clearly advantageous to have a design that operates effectively over a wide range of vibration frequencies. In order to solve this problem, several solutions have been studied like active/passive tuning techniques and widening of the bandwidth. In active/passive tuning techniques, simply the parameters of the generator such as the mass or the stiffness are altered so that the resonance frequency is tuned to match the environmental frequency. In the active tuning technique, this adjustment is done continuously, whereas in the case of passive tuning technique, the tuning actuators turn off after the adjustment. It was later showed mathematically [6] with some assumptions that active tuning techniques are not feasible because the tuning actuators will always require more power than the device can

generate. On the other hand, passive tuning techniques also require actuators and sensors, which increase the complexity and the cost of the device.

An alternative design would be a structure with a wider inherent bandwidth. Such a design can be done taking two different paths. The first alternative is to increase the system's bandwidth by increasing the system damping factor, this way the quality factor would decrease and the bandwidth would enlarge. Indeed, this approach widens the bandwidth response and the system is able to collect more energy in a wider range of vibration frequencies however, as the quality factor diminishes the system loses efficiency and consequently it worsens the peak response as demonstrated in Fig.2.20 [9]. The rise of damping factor allows a wider equivalent bandwidth but can also affect the peak output level resulting in lower energy capture effectiveness.

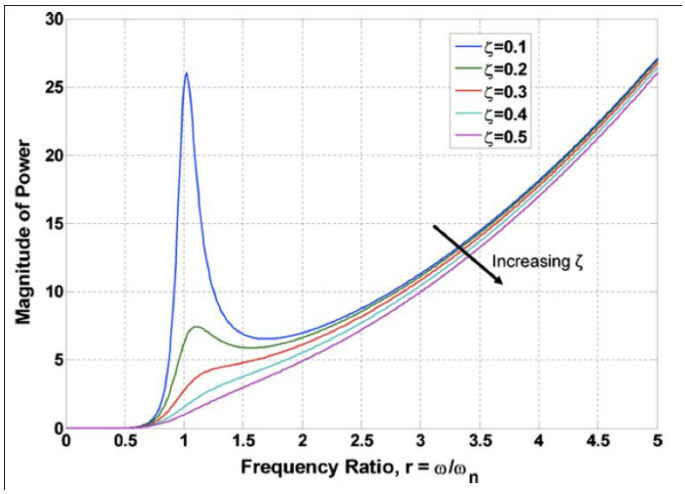

Figure 2.20 - Damping factor effect [6].

To overcome this limitation another process exists where multiple transducers with different frequency responses are combined granting improvement in power output and frequency flexibility. As it is shown in Eq. 2.14 the resonant frequency depends on several variables. Then in order to build a generator with the desired w_n it's possible to act in distinct ways. One way is to select the beam structural material by having a specific E, ρ and k and another option is to select the beam dimensions or the mass. MEMS technology is the technology in which these devices are usually integrated therefore the materials choice range is quite narrow although some material alternatives to silicon have been found [6] that permit adjustment of cantilever parameters due to it lower modulus of elasticity it is still hard to change the resonant frequency between several transducers only by changing the structural material. Given this, the simplest way to select the frequency between transducers is to correctly choose the beam dimensions or its mass.

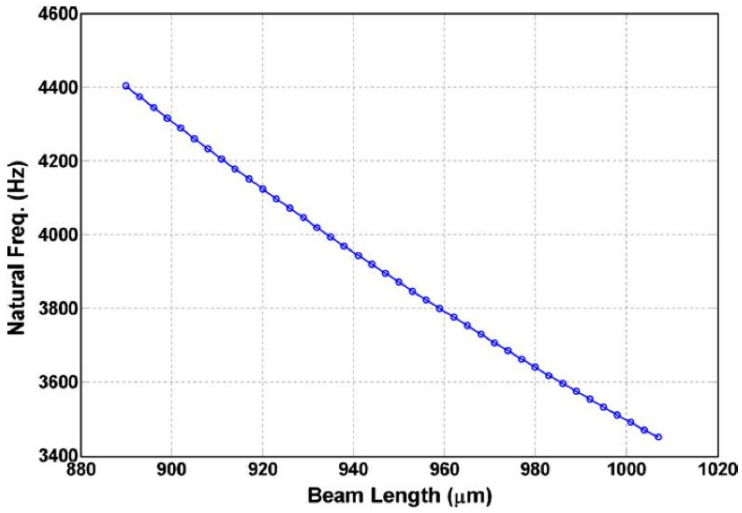

Figure 2.21 - Resonant frequency vs. Beam length [6].

The variation of these parameters is the base of a wideband transducer. By implementing a number of serially connected cantilevers with different lengths or different masses resulting in an array of cantilevers with different natural frequencies it is possible to build a generator that covers a wide band of external vibration frequency using the overlapping effect of resonance frequency. The design of such a device requires a chain of multiple beams each one with its own resonance frequency and a high Q factor resulting on a bandwidth that will cover the range of minimum to maximum resonance value of the array with high efficiency in each frequency value, Fig.2.22.

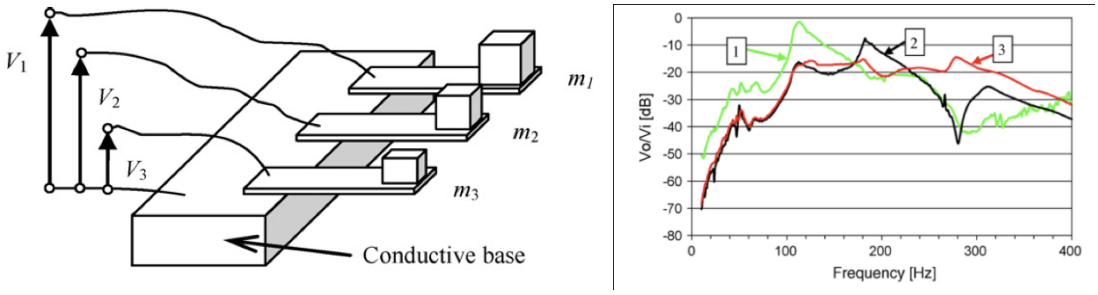

Figure 2.22 - Wideband system [3].

An example of a design is a wide bandwidth device implementation devices varying in length. This system is based in MEMS technology that ensures the production of cantilevers with various structure parameters. According to this design [6] the natural frequencies can be controlled by adjusting the beams lengths as shown in Fig.2.21.

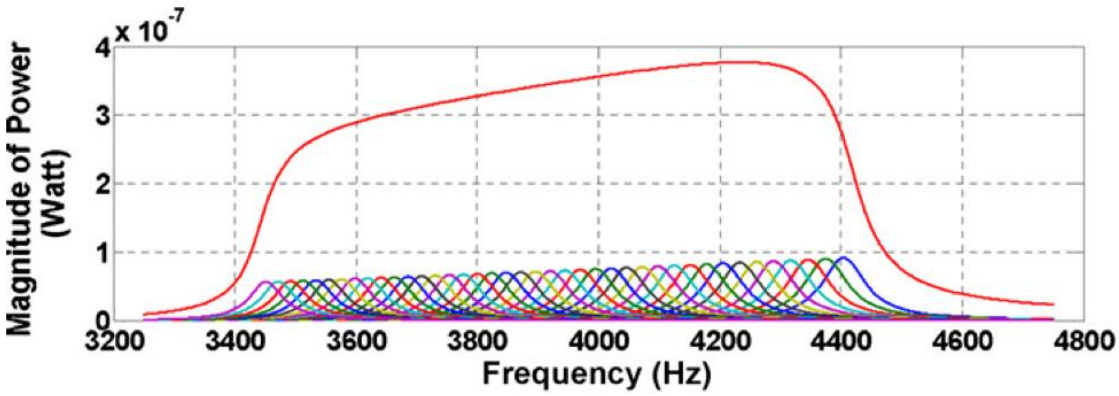

Figure 2.23 - Bandwidth of a 40 cantilevers array [6].

This way it is possible to select the cantilever lengths in order to match each device resonance frequency with the frequency values of the desired spectrum range. Fig.2.23 shows the estimated power output when forty cantilevers are used each one with a different length and consequently vibrating with maximum amplitude at different frequencies. The result is a wideband vibration-induced power generator device.

2.4 - Thermal Energy

Great amount of the world's power is generated by heat engines that convert heat to mechanical motion that can after be converted to electricity if necessary. These engines are not totally efficient and some part of the heat is always lost into the environment. Therefore, capturing this wasted heat energy and converting it into useable energy would have a tremendous environmental impact since it would increase the overall energy conversion efficiency. For example, the automobile exhaust waste can be captured and deliver energy to power or recharge the battery. This way the need for the alternator is reduced or even eliminated. Consequently, the load on the engine is reduced thereby improving fuel efficiency up to 10% [19].

Still, this energy is present not only in heat engines but it can also be found in the human body and so it follows natural to try harness this energy and convert it in electricity in order to power some sort of electronic system, to do so *thermoelectric generators* are used. These devices use the temperature difference between the human body and the environment to create electrical energy through *Seebeck* effect, a phenomenon in which a temperature difference between two materials produces a voltage difference and consequently, electrical energy.

2.4.1 - Thermoelectric Generators

Thermoelectric modules are based on the Seebeck effect, they are made from alternating p-type and n-type semiconductor pillars connected by metallic interconnects as pictured in Fig.2.24.When heat is applied to one side of a semiconductor, the charge carriers, electrons in the N semiconductor and holes in the P move to the cold end. This movement creates an open circuit voltage (V) proportional to the temperature difference (ΔT). The core element of a thermal energy harvester is the connection of an electron conducting (N-type) and hole conducting (P-type) material in series placed between a hot and a cold plate, this induces a net voltage that can be driven through a load, this array of thermocouples is known as thermopile. In order to optimize this device the thermopile other constitutive parts have to be properly designed, the power output depends on the distance between the plates as well as the pillar's high and width [17]. However, the efficiency of a thermoelectric converter also depends on the temperature difference $\Delta T = T_h - T_l$ (K) across the device.

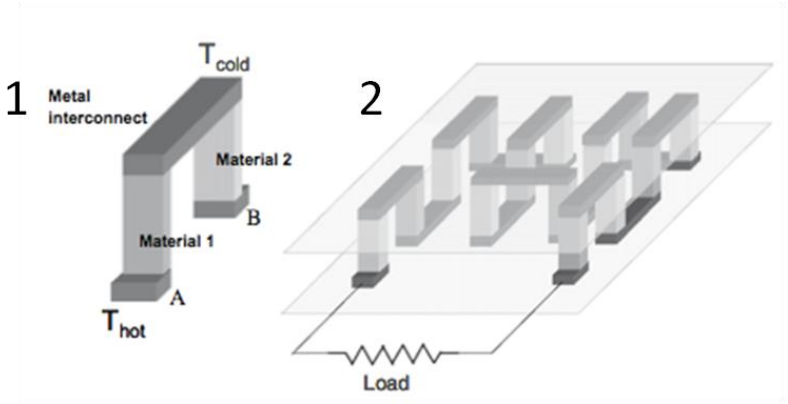

Figure 2.24 - (1) Thermocouple. (2) Thermopile [17].

This is because the thermoelectric generator, like all heat engines, can't have efficiency greater than that of a Carnot cycle (ΔT/Th). In other words, Carnot efficiency puts an upper limit on how well this waste heat can be recovered [21],

$$\eta = \frac{T_{high} - T_{low}}{T_{high}}, \tag{3.1}$$

Therefore, the energy extraction efficiency and consequently the power output is heavily related to the temperature gradient generated by the two environments.

The ability to fabricate exceedingly small semiconducting thermo elements has enabled the possibility of harvesting very small amounts of heat for low power applications such as wireless sensor networks and mobile devices [19]. An example of such a device is the Seiko's Thermic wristwatch, fabricated by EDM (Electrical Discharge Machining) [17] Fig.26.It is

constituted by ten thermoelectric modules [22] is capable of producing 22uW of electrical power with a 1.5K temperature drop and a 0.1% efficiency [19].An output voltage of about 300 mV was generated when the watch was worn [17] and although no longer in production, the thermoelectric wristwatch demonstrates the viability of utilizing thermoelectric in small power sources.

2.5 - Radio Frequency Energy

Although not visible, radio waves are all around us, emitted by a large variety of devices, from TV broadcast transmitters to garage door openers or wireless internet devices. These ambient radio waves can be used as a source of energy and despite being small the amount of power that can be skimmed off the radio waves can be enough for some applications such as microsensors or RFID *tags*. RF (Radio Frequency) harvesting converts the environmental radio waves into DC power. The power density levels up to the magnitude order of $3mW/m^2$ for a distance 25 to 100m, therefore it is not likely that radio waves produce enough ambient energy to power microdevices unless a large area is used for harvesting. Nevertheless, studies have been made and other techniques used and as example at a transmission power of 100 mW, values of 1.5 mW at 20 cm and 200 μW at 2m have been reported [17] which meaning that there is still space for progression in this field.

This energy harvesting method is accomplished by receiving radio waves with an antenna, converting the signal and conditioning the output power just like a common energy harvester system. The amount of power available for the end device depends on several factors including the source power, distance from the source, antenna gain and conversion efficiency.

2.5.1 - Faraday's Law

Faradays Law is the basic principle that allows harvesting RF energy and converts it into electrical power. In 1831 Michael Faraday discovered that a magnetic field could produce an electric current in wires that passed through the field, he called this induction and the law that governs it is known as Faraday's law. In practice, an electrical current will be induced in any closed circuit when the magnetic field through a surface bounded by the conductor changes, the generated current will be proportional to this change's rate.

As pictured in Fig.2.25 when a current flow in one coil a magnetic field is produced in the other coil but since the magnetic field is not changing according to the Faraday's law there will be no induced voltage in the secondary coil. But if the switch is opened to stop the current as in Fig.18 a change in the magnetic field will occur and a voltage will be induced.

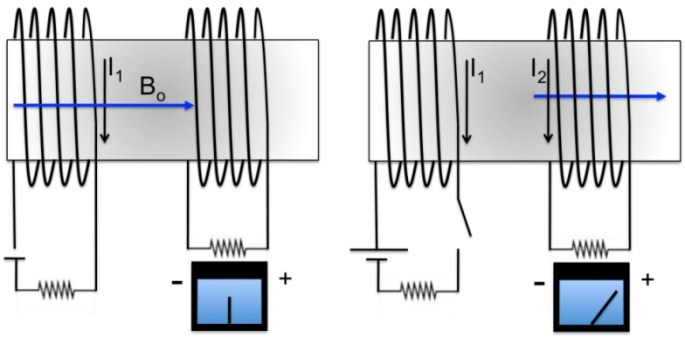

Figure 2.25 - Mutual inductance.

A coil is a reactionary device since it reacts to changes. The voltage induced will cause a current to flow in the secondary coil which tries to maintain the magnetic field as it was. Changing the magnetic field in the first coil produced a current in the second coil, this effect is known as Mutual Inductance. This effect is used in a *Passive RFID* system, when transferring data between the *Reader* and *Passive Tag* that uses the reader's coil or antenna power to perform the requested operation.

2.6 - Management Systems

Unlike common portable power sources where the average power they can provide is dependent on it lifetime, the energy provided by an energy scavenging source depends on how long the source is in operation or producing energy [23]. Generally, environmental energy availability and magnitude is unpredictable and variable over the time so, when available this energy needs to be converted and conditioned efficiently in order to reduce waste. In addition, environmental harvestable power is typically on the order of tens of microwatts [24], so it requires careful power management to successfully capture this small power amount. Recent improvements on energy management systems conversion efficiency created the possibility to power electronic using energy harvesting devices that are normally used in low power applications such as sensors and some sort of medical equipment.

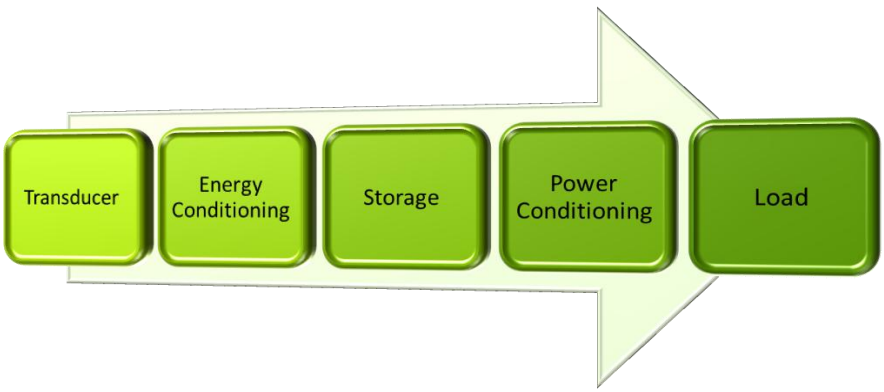

Figure 2.26 - Energy harvest system power management block diagram.

A classic energy-harvester system is represented in Fig.2.26 and it is constituted by five blocks, two of them are the power source -*Transducer* - and the application that can be seen as the load that consumes the produced energy, while the remaining blocks are responsible to control the energy flux in an waste less and effective manner.

The first block is the *Transducer*. It converts the present environmental energy into electrical energy. After produced, this energy is stored and conditioned by the next three blocks – the *Energy Management System* - this system should be able to adapt its input to the energy harvester and its output to the load.

The output energy from the *Conversion Electronics* is conditioned in way to properly charge the storage block, this operation depends on the energy source type. Vibration and RF energy harvesters produce an AC-output voltage so in order to use this energy the harvester requires first a rectifying AC-DC-converter stage. A second stage is needed in this block - a DC-DC converter –that converts the rectified collected energy into a usable format which is then delivered to the *Energy Storage* block electronics. In addition, the storage block must contain some sort of control system since the system has to shut down and ensure that it does not discharge the output when the harvester generates less energy than the energy used by the load [17]. The Energy Delivery unit in a general way provides the appropriate power supply to the load trough the use of supercapacitors or rechargeable batteries or both in simultaneously because of their complementary characteristics [14]. To enhance the system performance the harvest system electronics design shall incorporate micro-power devices in order to the energy consumed by the harvesting electronics doesn't overcome the generated energy by the input. Besides this, the energy leakage or loss in the storage and retention module must be the minimum possible.

This process holds great promise for low-power applications in a wide range of portable devices like mobile phones, wireless sensors and medical equipment as an alternative or batteries or even only to increase its useful life. Batteries have a finite life and are larger in size when comparing with energy harvester systems that have theoretically infinite life time and can be integrated in small systems using CMOS or MEMS technology.

2.7 - LTC3588-1 Energy Harvesting Power Supply

Among several power management devices [14] available, the Linear Technology microchip LTC3588-1 was the chosen one due to its power management features. Moreover, this new integrated power management system is small which makes it easy to integrate as well as cheap which makes it ideal to the project objectives and environment. Instead of making a detailed description of it operation [24] [25], it is going to be framed inside the *Energy Management System* description presented in the previous section.

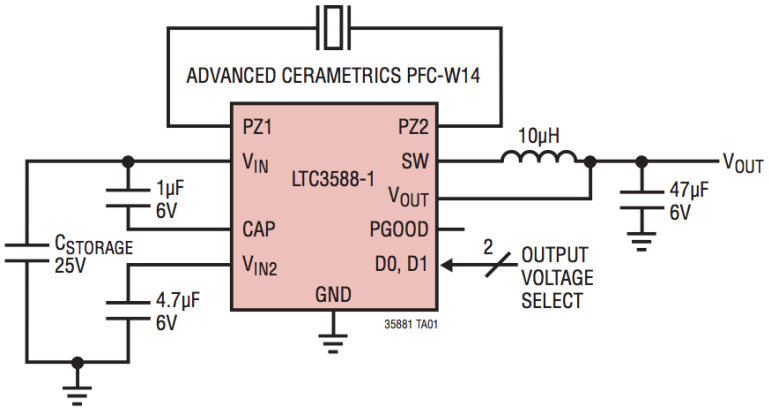

Figure 2.27 - LTC3588-1 [25].

The LTC3588-1 is designed to operate with several transducers technologies from Piezoelectric Vibration Induced to Thermoelectric generators and it can also be used in different configurations and porpoises or to power directly a microelectronic device or connected together with a common battery to increase it lifetime. It has four selectable output voltages (1.8V, 2.5V, 3.3V, 3.6V) and can drive a current up to 100mA and has an internal limiter up to 20V.

The *Conversion Electronics* of this system consists of two stages, the AD-DC and the Buck converter. The AD-DC converter is a low-loss full-wave bridge rectifier accessible via the differential inputs PZ1 and PZ2 inputs and rectifies AC inputs such as those from a piezoelectric element, Fig.2.27. This stage has a drop of about 400mV and is capable of carrying up to 50mA. Still, rectified DC voltage from the power generator needs to be converted to levels acceptable to recharge the *Energy Delivery* block and consequently power the *Application*, in order to do so a Buck or a DC-DC step-down converter is used. This unit constitutes not only the last stage of the *Conversion Electronics* block but also the part of the *Energy Delivery* block since in its final output the energy is ready to use by the *Application*.

The buck converter charges an output capacitor through an inductor and it does this by using two internal CMOS switches. The PMOS ramps the inductor current to a value slightly higher than the selected output which is then ramped down through the NMOS switch discharging the inductor's charge into the output capacitor. The capacitor smooths out the inductor current variations into a stable voltage at V_{OUT}, and efficiently delivers energy to the *Application*. To improve the efficiency of the DC-DC converter a capacitor between the gate and the source of the switching transistors is added [17], in this system's case one between V_{IN} and Cap and another between V_{IN2} and Ground. If both capacitors are charged up to the threshold voltage of the transistors, the buck is able to start conducting as soon as the input voltage starts to increase making this way a more efficient circuit. The capacitor placed between CAP and V_{IN} serves as gate drive for the PMOS switch while the other capacitor connected from V_{IN2} to Ground serves as gate drive for the buck NMOS switch. Obviously, a

management system such as this needs storage devices in order to use them as buffer reservoirs between the *Application* operation cycles and to better control the energy flux from the input to the output to so an input and an output capacitor shall be used. Input capacitor - $C_{STORAGE}$ – stores the resulting DC voltage from the rectifier bridge.

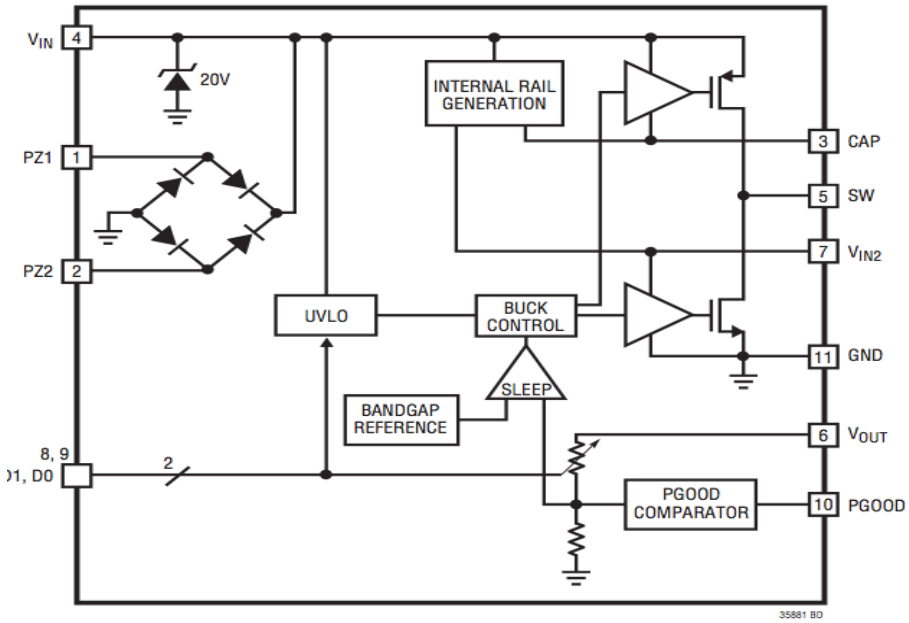

Figure 2.28 - LTC3588-1 block diagram [25].

When a load exists at the output the buck can efficiently transfer the available energy to the output capacitor - C_{OUT}. These two capacitors constitute the *Energy Storage* elements and they can be sized to support larger current loads. Despite all the elements described above can be classified as high efficient the core of the chip energy management efficiency is the *Energy Delivery* system. In Fig.30 the most relevant elements that constitute this system operation are represented, the Undervoltage Lockout (UVLO) and the Buck control. When the voltage on $C_{STORAGE}$ - V_{IN}- rises above the UVLO rising threshold the buck converter is enabled and charge is transferred from the input capacitor to the output capacitor, if the $C_{STORAGE}$ voltage is depleted below UVLO falling threshold voltage the buck converter is disabled. This is the first energy block control and is related to the input voltage level, the output energy state is controlled by the *Buck Control* together with the *Sleep* comparator represented in Fig.2.28. If the C_{OUT} voltage level matches the selected output voltage the converter enters in a low consumption sleep state that continuously monitors the output voltage using the sleep comparator. During sleep the *Application* energy is provided by the output capacitor until its level is under the required voltage. That is when the buck converter wakes up and again drives current to the output until it reaches the regulation voltage point. This operation flux is repeated and guarantees maximum efficiency management. Additionally, in order to better

interact with a microcontroller this microsystem integrates a control signal – *PGOOD* – designed to drive a I/O chip or a microprocessor. This signal produces a high logical value when the V_{OUT} level is above 92% of the regulation point and a low logical level when below. This signal is independent of the UVLO level since even if V_{IN} falls below UVLO falling threshold the PGOOD will remain high until V_{OUT} is depleted below the referred level.

Chapter 3

Near Field Communication

3.1 - Introduction

Near Field Communication (NFC) is a standardized short range communication technology that allows two-way interaction between electronic devices. It is based on RFID, so it uses magnetic field induction to enable communication between electronic devices in close proximity. NFC operates at the high frequency band 13.56MHz over a distance of only a few centimeters and with a short set-up time, which makes it inherently secure and a fast communication technology. It currently offers data transfer rates of 106 kbit/s, 212 kbit/s and 424 kbit/s.

There are several modes of communication defined by the ECMA-340 Standard and the NFC Forum specifications. According to NFCIP-1 standard there is the *Passive* and the *Active* mode while NFC Forum define three modes as well: *Reader/Writer*, *Peer-to-Peer* and *Card Emulation Mode*. The *Passive Mode* is particularly useful for devices that use batteries and need an efficient energy management and since the project device fits on the description it can clearly take advantage of this feature. Therefore the study will be focused on this transmission mode.

In order to understand what the technology behind NFC is a brief approach is done to RFID (*Radio Frequency Identification*). After it, we will dive in the NFC specifications and standards where the NFC operation is described in a detailed way.

3.2 - Radio Frequency Identification (RFID)

Radio Frequency Identification uses radio waves to automatically identify physical objects either persons, animals or ordinary items. It was created in order to overcome other Auto-ID (Automatic Identification) methods limitations such as bar code that has little memory capacity. RFID technology is able to support a large set of unique identifications.

A basic communication system using RFID technology consists of a reader or interrogator device and one transponder or tag. The tags are devices where the data is stored and the reader is the responsible for the communication initialisation by sending a signal, which is then replied by the tag with the requested information. At highest level we can divide a RFID system in two classes: *passive* and *active*, the factor that differentiates it is the type of *tag* used.

3.2.1 - Frequency bands

RFID systems are classified as radio systems since they radiate electromagnetic waves. The radio spectrum is regulated with great difference between different continents and even different countries. The RFID frequency classes are present in Table 3.1.

Table 3.1 - RFID frequency classes

Designation	Range
Low frequency (LF)	30kHz-300kHz
High frequency (HF)	3MHz-30MHz
Ultra high frequency (UHF)	300MHz-1GHz
Microwave frequency	> 1GHz

The most common frequency for RFID systems is 13.56MHz (HF). This range is accepted worldwide and the components of such transponders are easy and cheap to manufacture.

3.2.2 - Tags

Passive tags don't require an on-board power source such as a battery, this class of tag uses the energy emitted from the reader to power itself and transmit its stored data to it. Due to its simple construction these devices don't require maintenance, have an indefinite operational life, are small enough to fit into an adhesive label and are also cheaper than the other *tag* class. A passive tag is constituted by an antenna and a microchip. The antenna objective is to draw energy from the reader's signal to energize the tag as well as send and receive data from the reader. It is physically attached to the microchip which rectifies the drawn AC power to DC and transmits the requested data to the reader. The data is stored in the microchip memory and is modulated also by the microchip into a signal to be transmitted to the reader. A *passive* RFID system uses passive tags, in this system the reader is the responsible to always initiate the communication powering the passive tag and collect the data stored in the *tag*.

Active tags do not need the reader's emitted power for data transmission due to its on-board power source, thus it can broadcast data to its surrounding even in the absence of a reader. Due to this property, it can also be called a transmitter. Another type of active tag known as transponder (*transmitter/receiver*) enters a sleep state in the absence of a reader in order to save battery power and reduce the amount of RF noise in its environment. Although these types of tags improve the utility of the device its maintenance costs are higher and the useful life is shorter when compared to passive tags. The parts that constitute an active tag are the same as a passive but with one more component – the on-board power supply. The main advantage of active tags is the wide variety of tasks they can perform: monitoring, control, sensing and so on. The communication of an active RFID system can be initiated by the active tag and does not need the reader to energise it and start the data interchange.

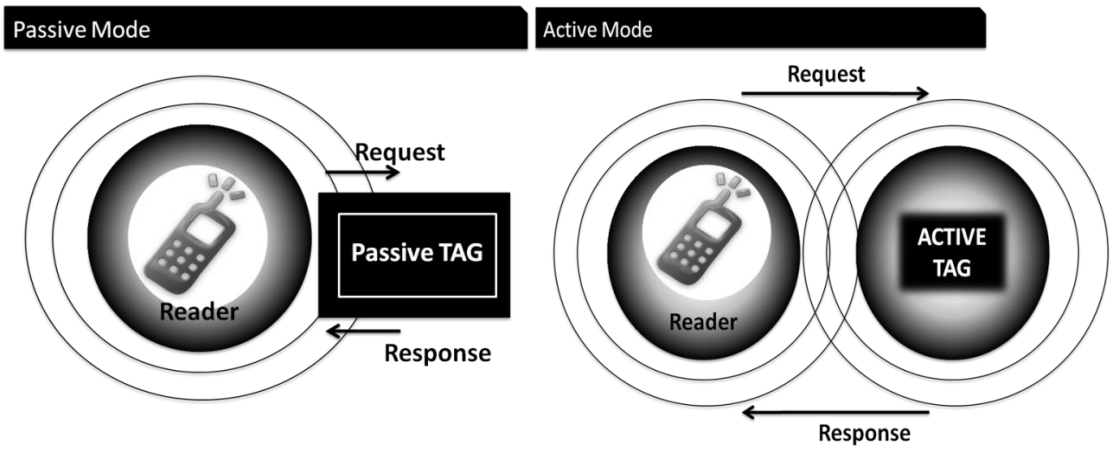

Figure 3.1 - RFID Passive and Active mode.

3.2.3 - The Reader

Also known *interrogator*, this device can read and write data to RFID tags. Its main components are: a receiver, a transmitter, a microchip, memory and the power. The transmitter is used to transmit AC power to the tags in its read zone while the receiver receives the tag's signals and route it to the microprocessor. These two blocks make the interrogator's main structure - the *transceiver*. The reader has its own power source in order to power the device electronics such as the microchip and the memory. Data is received and processed by the microchip and converted into a digital format that is stored in the memory.

Figure 3.2- RFID passive tag and reader.

3.2.4 - Power

The passive tags have no power supply of their own, instead they use the induced current from the field generated by the reader to process the information and send a reply. If a second coil is located in the vicinity of a first coil will be affected by the magnetic field generated by it and a portion of energy will flow through the second coil. This energy connects the two coils inductively – Mutual Inductance, this property is described in the previous chapter. This is the principle upon the RFID passive tags systems are based and is used for both power and data transfer. If the coupling is insufficient a capacitor may be connected in parallel with the antenna to be used as a reservoir of charge that can be used to power the tag chip. However, in the high frequency band systems the input capacitance of the microchip together with the parasitic impedance of the coil is sufficient.

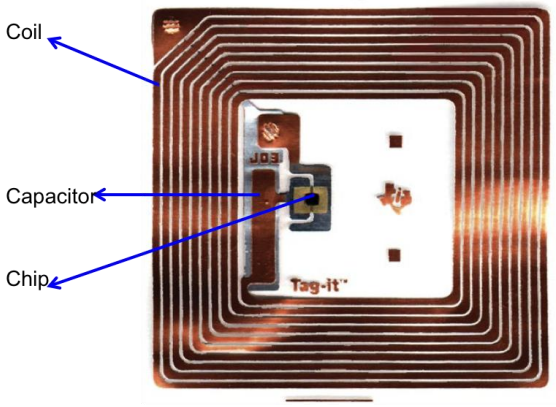

Figure 3.3 - RFID passive tag.

3.2.5 - Data Transfer and Modulation

The modulation technique used by close-coupled systems such as passive RFID is *load modulation* to uplink (tag to reader) and ASK to downlink (reader to tag) [20]. Load modulation makes use of the short distance between the reader and the transponder coil and the mutual inductance effect. When the reader antenna or coil generates a signal the nearby

transponder is magnetically connected to the reader through its antenna coil. A current is drawn in the transponder coil and will give rise to its small magnetic field, which will oppose to the reader's field. The reader antenna can detect this as a small increase in current flowing through it, which is proportional to the load applied to the tag's coil. This allows communication between the tag and the reader by simply varying the load applied to the transponder. The tag's electronics applies a load to its own antenna coil and varies it over time, a signal can be encoded as tiny variations in the magnetic field strength representing the tag's data. Then the reader can recover this signal by monitoring the change in current through its coil and then process and store it as digital data.

A used approach for systems in this frequency is to first modulate a subcarrier with frequency f_s, and then use the subcarrier to modulate the main carrier with frequency f_c. Resulting in a modulation product where the data is located, see Fig.3.4.

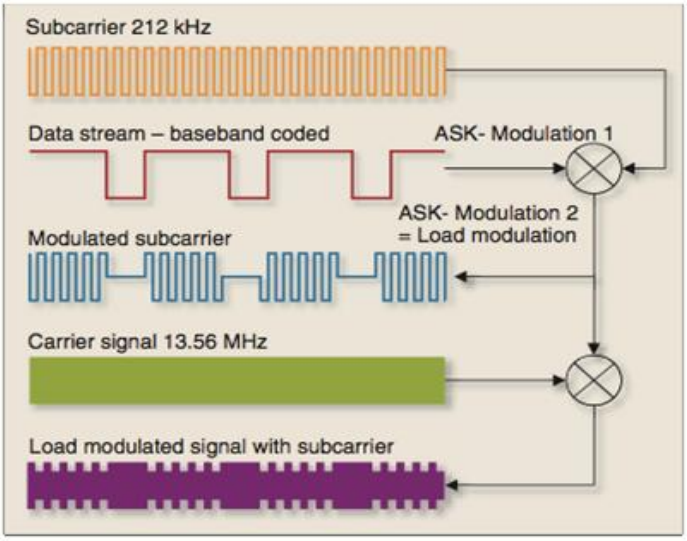

Figure 3.4 - RFID modulation scheme [20].

The modulation techniques for subcarrier modulation are amplitude shift keying (ASK), frequency shift keying (FSK) and phase shift keying (PSK).The ASK is realized by changing the amplitude of the signal to transmit between two values where A is the high value and B is the low. The modulation index is measured as it follows: M = (A+B)/(A-B). The frequency shift keying consists in switching the frequency between two values of the signal to be transmitted. Each one of the frequencies represents a ONE or ZERO. PSK does not change the amplitude or frequency of the signal to transmit but instead the phase. The phase is switched between 0 and π that represents the data.

3.3 - RFID and NFC

To better understand the NFC innovations and the main characteristics we compare it to RFID, analyzing the requirements and the advantages of each one and defining processes that each technology offers.

NFC was deliberately designed to be compatible with RFID tags operating in this band. NFC systems consist of two elements: the initiator (called reader in RFID) and the target (called tag in RFID). While the first begins and controls the information exchange the second is the device that responds to the requirement of the initiator. According to the *ECMA-340* standard, in an NFC system there are two modes of operation: Active and Passive. In the active mode, both devices generate their own field of radio frequency to transmit data (*peer to peer*). In the passive mode, only one of the communicating devices generates the radiofrequency field, while the other uses load modulation to realize data transfers.

One of the characteristics that distinguish these two systems is the fact that the NFC devices, unlike RFID, can work as Initiator or Target, which allows the NFC devices to be mobile, Fig.3.5 (A). In this case the data can be contained within the initiator itself. An RFID reader or is fixed or is a mobile device with big dimensions because of the necessity to be attached to a computer to feed and read the tag. This fact limits the extent of which a change of place can be carried out, Fig. 3.5 (B). Normally, the antenna is located in one place and the tags are completely mobile while the NFC devices can move around freely designing a completely different and more flexible communication scheme.

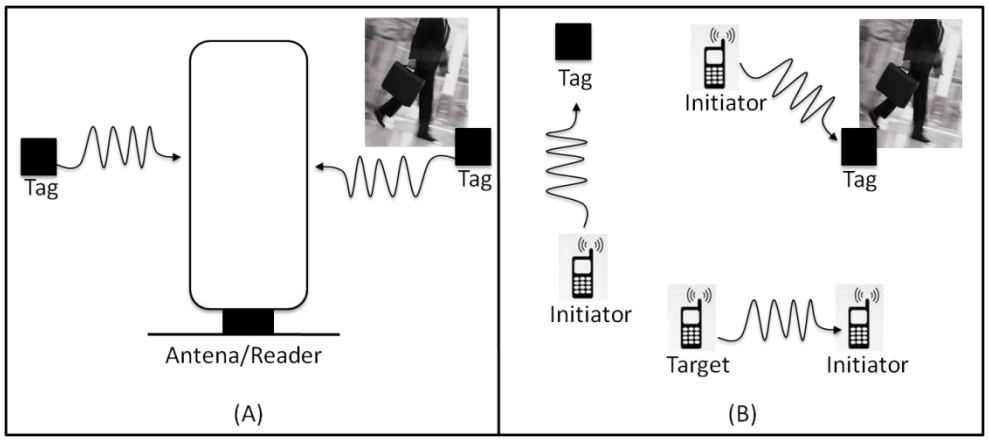

Figure 3.5 - Mobility comparison between RFID and NFC.

It's also important to refer the distance in which the devices operate from each other in both technologies. Assuming the RFID tags as active the distance to detect an NFC device is quite small compared to an active RFID tag that can be detected in some cases at dozens of meters. This is a disadvantage of the NFC technology, but on the other hand is itself a security factor. It ensures that we can always be aware of our proximity to a device and that the signal can't be intercepted without being noticed by the user. Unlike RFID active tags,

this physical proximity of the device and the reader gives the user the reassurance of being in control.

3.4 - Standards and Specifications

NFC is a simple extension of the ISO/IEC 14443 proximity-card standard that combines the interface of a smartcard and a reader into a single device. Because NFC is compliant with this standard it is compatible with millions of contactless smartcards and readers in use worldwide. Near Field Communication standards were approved in 2003 with ECMA-340 and ISO/IEC 18092. These standards specify the modulation schemes, coding, transfer speeds and frame format of the RF interface of NFC devices, as well as initialization schemes and conditions required for data collision-control during initialization-for both passive and active NFC modes.

Another stage in the standardization process came when Nokia, Sony, and Philips formed the NFC Forum in 2004. This non-profit forum tries to educate the market about NFC by promoting implementation and standardization of NFC technology to ensure interoperability between devices, services and protocols. In 2006, this forum formally outlined the architecture for NFC Technology and released some specifications, which can be used as guidelines by other companies to create their own products. NFC Forum now has 140 members and has released 12 specifications.

3.4.1 - ECMA Standards

There are nine ECMA Standards oriented to define and standardize NFC technology. Some of them define the way they communicate and operate and others define test methods. To have a general idea, in Table 3.2 is presented the existing standards with the code number and it designation.

3.4.1.1 - ECMA 340

This standard defines communication modes for Near Field Communication Interface and Protocol using inductive devices operating at the frequenccy of 13,56MHz as well as defines both Active and Passive communication modes. Among other specifications ECMA – 340 defines modulation schemes, codings, transfer speeds and conditions required for data collision control during initialization.

3.4.1.1.1 - Modes

In the Active communication mode both the Initiator and the Target use their own RF field to enable the communication, Fig.3.6. While the Initiator starts the communication, the Target responds its command by using its self-generated RF field.

Unlike the Active mode, in Passive communication mode the Target responds to the Initiator using a load modulation scheme like a RFID system, Fig.3.1. These modes shall not be changed until the Target is removed from the Initiator RF field or being deactivated. In the Passive mode the Target operates continuously between H_{min} (1.5 A/m) and H_{max}(7.5A/m), rms value. All readers and active transponders should be able to generate an RF field of at least H_{min} and to avoid collisions, all devices must be able to detect a RF field with the minium field strength $H_{threshold}$= 0.1875 A/m at 13.56MHz – carrier frequency (f_c).

Wathever mode the devices are operating on, they must support communication using three bit rates: 106kbp/s, 212 kbp/s and 424 kbp/s which is chosen by the Initiator that starts the communication.

Table 3.2 – ECMA standards.

ECMA	Designation
340	NFC Communication Interface and Protocol (NFCIP - 1)
352	NFC Communication Interface and Protocol (NFCIP - 2)
356	NFCIP – 1 - RF Interface Test Methods
362	NFCIP – 1 - Protocol Test Methods
373	NFC Wired Interface (NFC - WI)
385	NFC-SEC: NFCIP – 1 - Security Services and Protocol
386	NFC-SEC 01: NFC-SEC Cryptography Standards using ECDH and AES
390	Front-End Configuration Command for NFC-WI (NFC-FEC)
391	Memory-Spot Interface and Protocol (MSIP - 1)

3.4.1.1.2 - Modulation – Initiator to Target at 106 kbp/s

The bit rate for transmission during initialisation and single device detection from the Initiator to the Target is 106kbp/s and shall use ASK modulation with a modulation index of 100% to generate an impulse – Pulse - as shown in Fig.3.6, the pulses values are presented in Table 3.3. Moreover, the type of byte encoding applied is least significant bit first.

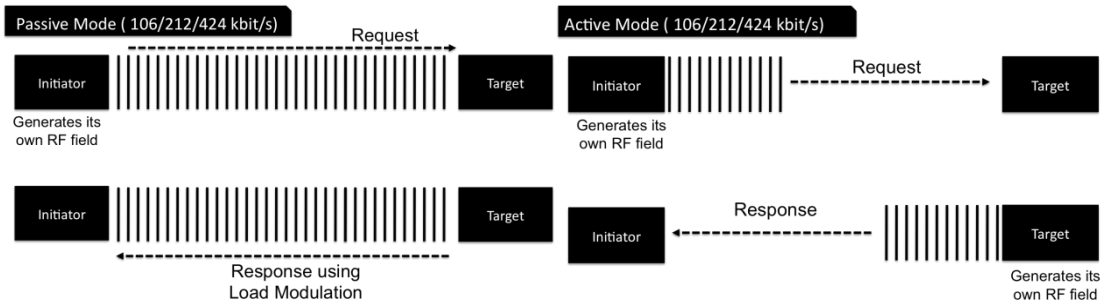

Figure 3.6 - NFC passive and active modes.

The envelope of the field decreases to below 5% of the initial value $H_{INITIAL}$ and remains at his value for a period longer than t_2. Overshoots shall remain 90% and 110% of $H_{INITIAL}$. Then, the target detects the End of Pulse after the field exceeds 5% of $H_{INITIAL}$ and before it exceeds 60% of $H_{INITIAL}$. The time between these two values is defined by t_4. This definition apllies to all modulation envelope timings.

The NFC standard specifies the following coding and bit representation when transferring data.

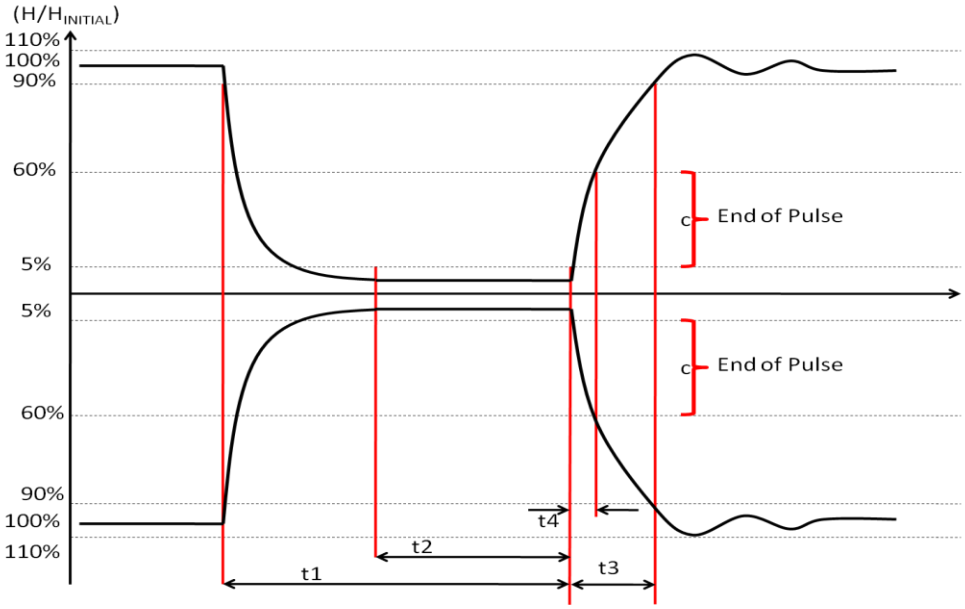

Figure 3.7 – Characteristics of a NFC communication pulse [1].

The communication start should begin with a Pulse at the beginning of the bit duration. ONE is represented with a pause at the second half of the bit duration. ZERO is represented with no modulation for the whole bit duration with the following two exceptions:

→ If there are two or more contiguous ZEROs, from the second ZERO, a pulse must occur at the begining of the bit duration.

→ If the first bit after the start of communication is zero, a pause will occur at the begining of the bit duration.

Table 3.3 – Pulse times values.

Pauses length (Condition)	t1 (μs)	t2(μs)		t3(μs)	t4(μs)
		(t1≤2.5)	(t1> 2.5)		
Maximum	3.0	t1		1.5	0.4
Minimum	2.0	0.7	0.5	0.0	0.0

3.4.1.1.3 - Modulation – Target to Initiator at 106 kbp/s

The modulation from Target to Initiator is different as the Target has to couple inductively with the Initiator. The carrier frequency is loaded to generate a subcarrier with frequency 847.5KHz (f_c/16). The modulation is accomplished by switching a load modulation in the target using this subcarrier.

The subcarrier is modulated using Manchester coding for bit representation as shown in Fig.3.9.

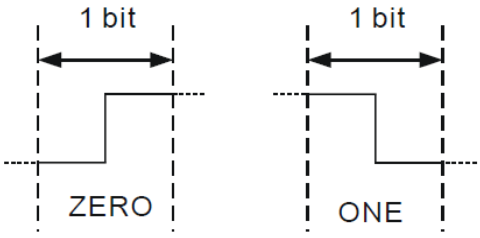

Figure 3.8 - Manchester bit encoding (obverse amplitude)

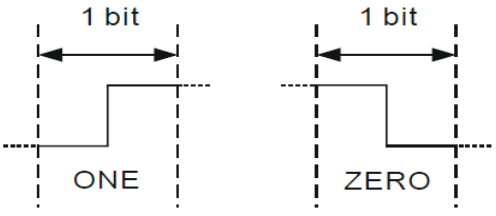

Figure 3.9 - Manchester bit encoding (reverse amplitude)

Manchester coding with obverse amplitudes shall be used. That means that the binary Manchester symbol ZERO has low amplitude for the second half of the bit duration and high amplitude for the second half of the bit duration. Symbol ONE is represented the other way, shall have high amplitude for the first half of the bit duration and low amplitude for the second half of the bit duration. Reverse polarity in amplitude is not permitted.

3.4.1.1.4 - Modulation – Initiator to Target at 212 kbp/s and 424 kbp/s

The modulation scheme from the Initiator to the Target when using other bit rates - 212 kbp/s and 424 kbp/s – differ from the lower bit rate – 106 kbp/s. Despite the modulation is still ASK, its index is now between 8 % and 30 % of the operating field. The modulation waveform must comply with Fig.3.10.

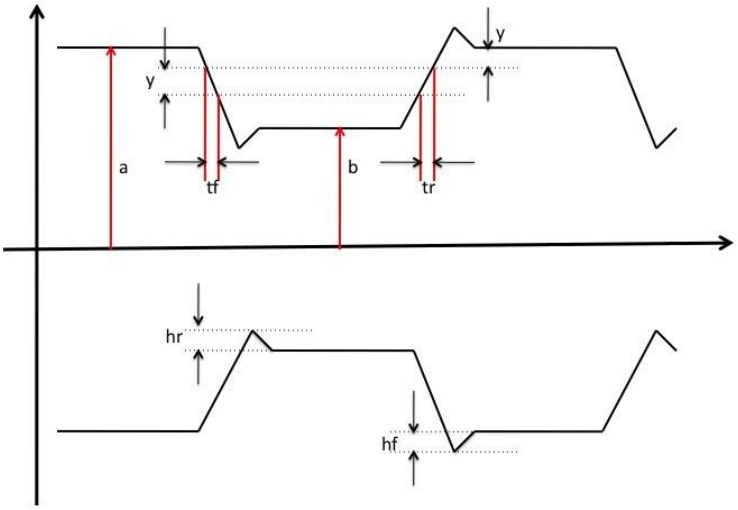

Figure 3.10 - Modulated waveform [1].

The rising and falling edges of the modulation shall be monotonic and the transmission during initialisation and single device detection is the same. The peak and minimum values of the modulated signal are defined by a “a” and a “b”. When transferring data using bit rate 212 kbp/s or 424 kbp/s, the NFC standard specifies that Manchester bit coding should be employed. Reverse polarity in the amplitude is permitted and the byte encoding is most significant bit first.

3.4.1.1.5 - Modulation – Target to Initiator at 212 kbp/s and 424 kbp/s

With the highest bit rates the Target responds the same way as in 106kbp/s case. The difference is that the subcarrier modulation is not used and instead it is accomplished by switching the load, generating Manchester coding. The load modulaton amplitude must be at least $30/H^{1.2}$ (mV peak) where H is the (rms) value of magnetic field strength in A/m and the byte enconding is most significant bit first.

3.4.1.1.6 - General Protocol Flow

An NFC device can be either in target mode or initiator mode, the Passive devices are always in Target mode per default and may switch to Initiator mode if required by the application. When in Target mode the device shall wait silently for a command from the Inititator or in other words an externally generated RF field to activate.

If in Initiator mode the device performs initial collision avoidance by detecting external RF fields before activating its own. If no RF field is detected the process flow proceeds and the application decides in which communication mode it will operate - Active or Passive. If passive, it must perform a single device detection before the transfer starts.

3.4.1.1.7 - Colision Avoidance

When initalizing a transmission the Initiator must detect when at least two Targets transmit simultaneously. Mechanisms to perform this detection are specified for NFC. Devices generating RF fields like the Initiator, do initial collision avoidance by sensing the carrier for already existing RF fields. If an RF field stronger or equal to $H_{threshold}$ is detected, the RF field is not switched on If no RF field is detected within a time period of $T_{IDT} + n \times T_{RFW}$, *where* T_{IDT} (initial delay time) > $4096/f_c$, T_{RFW} (RF waiting time) = $512/f_c$ and n is a random generated integer between $0 \leq n \leq 3$, the RF field is switched on. The initiator then waits T_{IRFG} (initial RF guard-time) > 5 ms before starting to transmit a request.

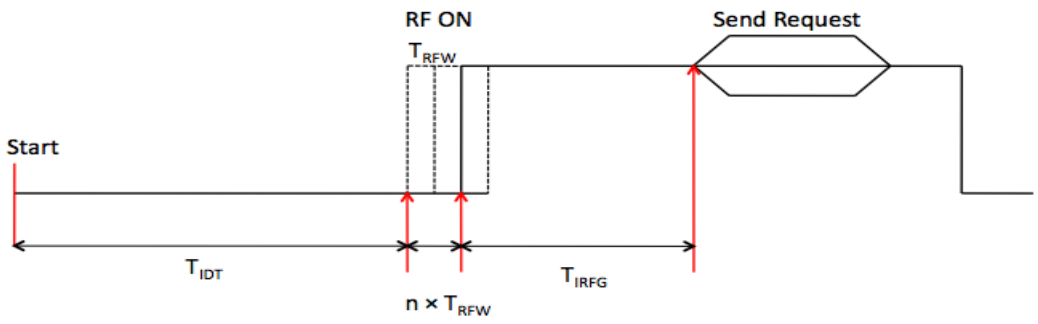

Figure 3.11 - Initial RF Collision Avoidance [1]

3.4.2 - NFC Forum Specifications

3.4.2.1 - Tags

According to NFC Forum, NFC tags are devices with the same operating principle as in an RFID system. They are passive devices that can be used to communicate with active NFC devices such as an active reader/writer device. In order to define the communication between tags and the active devices, the NFC forum introduced some Tag specifications. These NFC tag type formats are based on ISO 14443 Types A and B which is the international standard for contact-less smartcards and Sony FeliCa [30] which conforms to ISO/IEC 18092, the passive communication mode, standard.

There are four types of Tags defined, what distinguish them is their memory capacity and the different mode they can operate. While the Type 1 and Type 2 tags may be either read/write or read-only the Type 3 and 4 are read-only.

3.4.2.2 - Technology Architecture

The NFC Forum specifications define three communication modes: Reader/Writer, Peer-to-Peer and Card emulation mode. The Reader/writer mode is capable of reading or writing an NFC tag. The peer-to-peer mode allows two NFC devices to exchange data between them while the Card Emulation mode the NFC device acts as an NFC Tag, appearing to an external reader the same as a traditional contactless smart card. The first two modes use ECMA-340 active communication mode due the generation of an RF field by at least one of the devices, the Card Emulation Mode is in Passive Communication Mode as its RF field is never generated, Fig.3.6.

NFC Forum also defines the Analogue Specifications, the Digital Protocol Specification and the NFC Activities Specification. The first specifies the radio frequency characteristics and the operating range of the devices while the second defines the building blocks for communication and the implementation of ISO/IEC18092 and ISO/IEC 14443 digital aspects. The NFC Activities Specification defines activities required to set up communication in an interoperable manner, based on the building blocks of the digital protocol specification. In the Card Emulation Mode the specifications will deal with proprietary contactless card applications based on 14443 A/B or Felica [30].

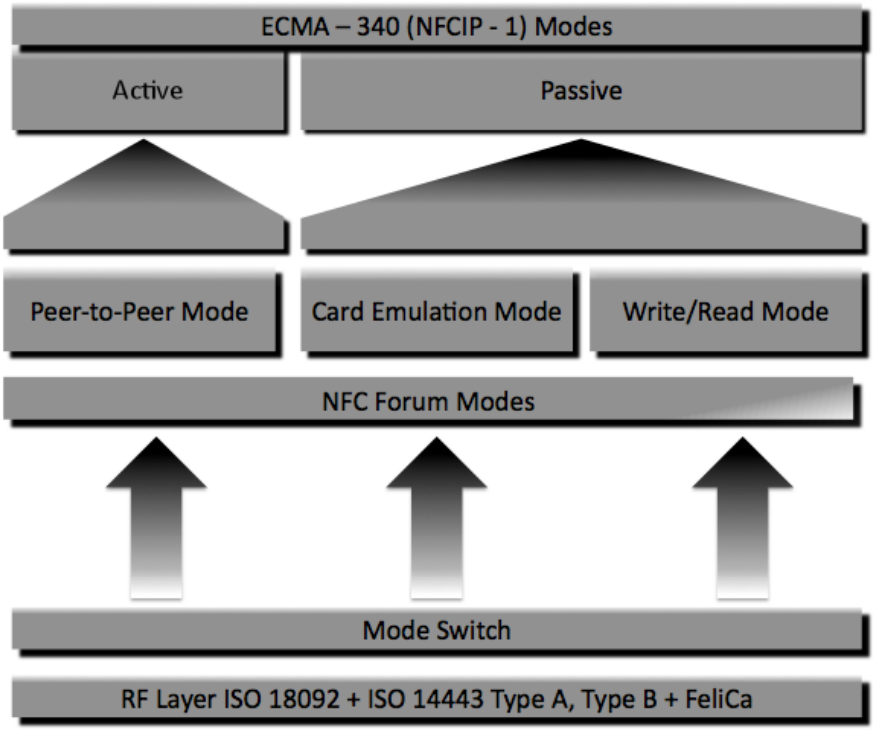

Figure 3.12 - NFC standards and specifications relationship.

3.5 - Low Power

Taking into account one of the research objectives – the device low consumption – it follows natural to fit this communication technology in this context. Regarding the NFCIP-1 operation modes, the Passive mode is the one that guarantees the minumum overall consumption. Since in this mode one of the devices does not generate its own RF field it does not spend as much energy as if it was communicating in Active mode. Moreover, considering the diverse data transfer rates: 106, 212 and 424 kbp/s it is also possible to relate it with the device consumption. For each bit transmission exists an inherent energy consumption peak. Given this, it is obvious that with the slowest bit rate each peak duration is bigger comparing it with the fastest bit rate. Consequently, with the fastest speed rate of 424 kbp/s the lowest consumption rate is achieved.

Chapter 4

Power System

4.1 - Introduction

The first stage of the research was to study a proper way to power the system in order to guarantee a good performance regarding the project objectives. Given this, it was taking into account one of the project's aims, integrate the device into a portable device meant to be used in the the user's wrist. Therefore, putting together an empirical analysisis with the environmental energies presented it is easy to conclude that one of the solutions would be to harvest the vibration energy generated by the user's wrist motion and feed the device electronics. Moreover, according to some literature it is possible to capture 0.33 W of energy from the human arm motion [21]. To do so, a piezoelectric trandsucer is the converter that best suits in the device characteristics, not only due to ease of integration but also due to the nature of the mechanical energy.

To know exactly the power generator capabilities as well as to find out if in fact it produces enough energy to feed the device several tests were made. In this chapter the description and results of these tests are presented as well as the conclusions. In adittion, other ambient energies were also study targets, and these brief tests are also exposed.

4.2 - Power Budget

Measure the piezoelectric generator power output is essencial to draw conclusions about the viability of this system. However, to know if the energy produced is enough it is necessary first to know how much energy will the device consume. As referred, the final product will be able to communicate through several communication protocols such as NFC. Therefore, to communicate the system will integrate an NFC communication microchip and to control all the communication and operation procedures within the device a microntroller is used. The *NXP PN532* microchip is responsible to ensure the NFC communication while an

ATMEL microcontroller is in charge of the control, the *ATMEGA1284P*. At this point, knowing how much will these two elements consume is a priority, part of this information is presented in Tab.4.1 and Tab.4.2. Although both units have different power modes they can be divided into two main goups: sleep and active mode.

Table 4.1 - NXP PN532 current consumption characteristics.

Mode	TYP	MAX	Unit
Hard Power Down		2	μA
Soft Power Down	25	45	μA
Total Supply Current		150	mA

So, in order to evaluate the power budget value let's take in consideration these modes. For the PN532 there are two sleep modes: Hard Power Down and Soft Power Down. What differentiates these two modes is the RF detector, while in the first mode the unit turns off its RF detector and consequently can't detect if a device is trying to communicate the second mode has the RF field detector on. Given this, the sleeping mode that best fits in the device objectives is the Soft Power Down. When communicating the microchip is in active mode, consuming more current, the device is Total Supply Current mode. For the budget it's assumed that the device will have the proper antenna tuning which will make it consume less than 100mA. In addition, each NFC transmission lasts 20 ms which means it will consume around 100mA during this time.

Table 4.2 - ATMEL1284P DC characteristics.

Mode	Condition	TYP	MAX	Unit
Power Supply	Active, 4 MHz, V_{CC} = 3V	1.4	2.7	mA
	Idle, 4 MHz, VCC = 3V	0.25	0.7	mA
Power Save	32 kHz TOSC enabled, VCC = 3V	0.6		μ A
Power Down	WDT disabled, VCC = 3 V	0.17	2.0	μ A

As for the ATMEL controller, other options can be taken into consideration since it has more power mode options. In active mode let's consider he is working according to the Power Supply Active conditions. Relatively to the sleep modes, in order to make a realistic budget the maximum value of Power Down mode was the chosen one.

Concluding, according to this estimation the device will consume 47uA in sleep mode while in active mode it will have a 100mA load.

Table 4.3 - Power budget.

	SLEEP	ACTIVE
TOTAL	47 μ A	100 mA

4.3 - Tests

These performed tests have as main objective to quantify how much power can exactly a piezoelectric generator deliever. However, this tecnhology can not operate only by itself, therefore it needs a power management system which guarantees the convertion from mechanical energy into useable energy. Given this, the piezoelectric generator must be connected to the LTC 3588 microchip and together with it constitute the basic elements of the test plataform.

The piezoelectric generator used is a *Volture Piezoelectric Vibration Energy Harvester*. This bimorph structure has a 30-140 Hz bandwidth and it's designed to work with industrial vibrations, it is represented in Fig.4.1. Due to economic reasons it was not possible to use another piezoelectric element that would better fit the project's porposes. The ideal generator would have a lower bandwidth corresponding to the human arm motion frequency and a reduced size in order to better integrate it in a small portable device.

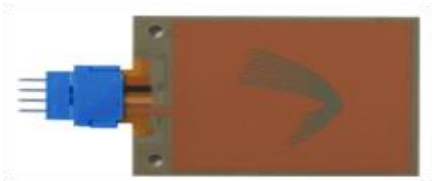

Figure 4.1 - Piezoelectric generator.

The other element is the management system. In order to be used it needs to be integrated into a PCB board. Following the device's datasheet, the schematic presented in Fig.4.2 was designed. The D0 and D1 outputs are connected both to high level which means that the selected output voltage is 3.6V. The next step was to design the physical board, the

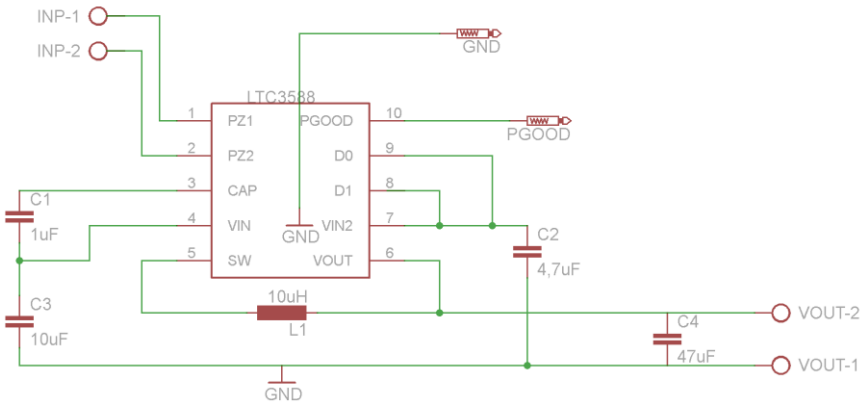

Figure 4.2 – LTC-3588 PCB schematic.

resulting design is shown in Fig.4.3. The piezoelectric power output can be connected to the board *INP* connection while the final energy is present at *VOUT* output. Besides these two connections there is also the PGOOD signal that can also be measured in the corresponding connector.

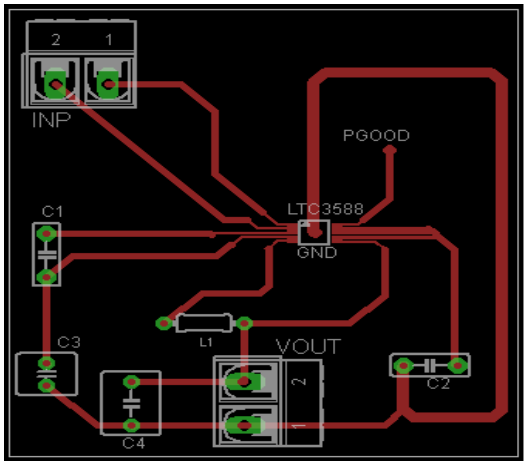

Figure 4.3 - LTC-3588 board.

Finally, after properly connected, these two units are connected to an oscilloscope in order to measure the board outputs. The *VOUT* is connected to channel one, while the *PGOOD* is connected to channel two. This way, it is possible to see not only the energy output values but also the behaviour of the PGOOD signal.

4.3.1 - General Description

Figure 4.4 shows each one of the test platform stages. In the first stage a manually induced vibration is applied to piezoelectric generator which consequently leads to an energy generation that is then captured by the management system. After properly conditioned, the energy is available in the LTC microchip output. From this point there are two changing variables: the output load and the output capacitor. The variation of these two factors will

provide crucial information about the abilities of the power system. By changing the output load it is possible to test the power system response for the two power budget modes: active and sleep. On the other hand, the output capacitance is changed in order to verify how the system will react to a bigger output energy reservoir.

4.3.2 - Specific Description

The first aim is to know the amount of power the piezo can actually deliver as well as the order of magnitude of the induced vibration. The piezoelectric generator pulse print screen obtained in the oscilloscope is represented in Fig.4.5 where it is visible that the generator can deliver almost 20 V of peak voltage and the vibration frequency is around 4.5 Hz. After these measurements, the power system capabilities tests begin. The first tests were related to the Sleep MODE, therefore the lowest load is applied in the output and tested with two different output capacitors: 47µF and 2200µF.

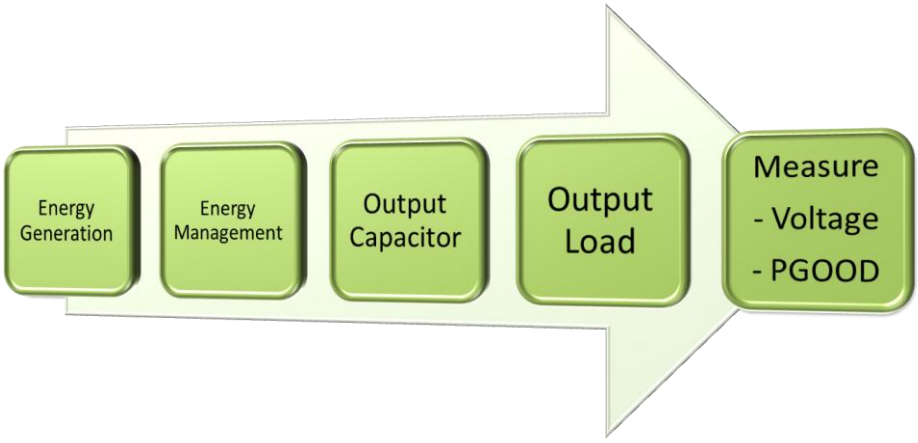

Figure 4.4 - Test platform.

The test represented the measurement of the t_{charge}, this time measures the interval between the beggining of the vibration and the moment that *PGOOD* is high. Next, the Active MODE is studied and the same method is followed but this time an higher output load is used. One of the results is presented in Fig.4.6. All these tests were done twice, one time with the energy vibration energy on the input and another without it. This way it's possible to know the system response to a situation where no displacement occurs.

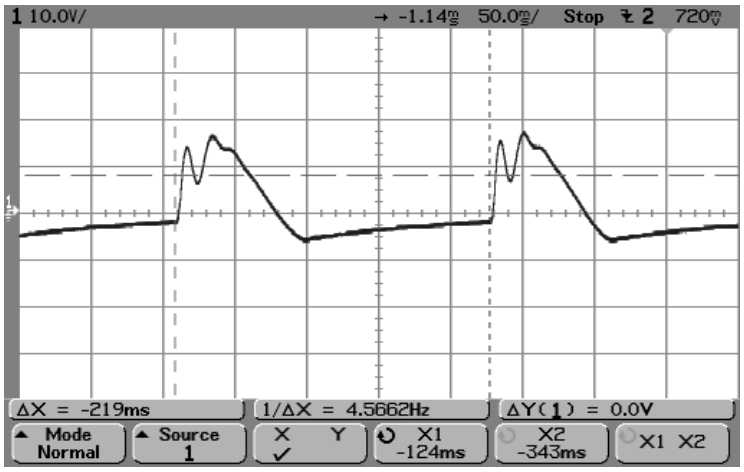

Figure 4.5 – Piezo generator signal.

Moreover, it is noticeable in these pictures the behavior of the PGOOD signal, which gives an indication that the energy management system is working properly. It is also important to refer the charging conditions. All the charging times were measured with the output load on except when using the highest load, as the energy wasn't enough to charge the output capacitor a power source was used. This way, the discharge curve using the bigger load can also be studied.

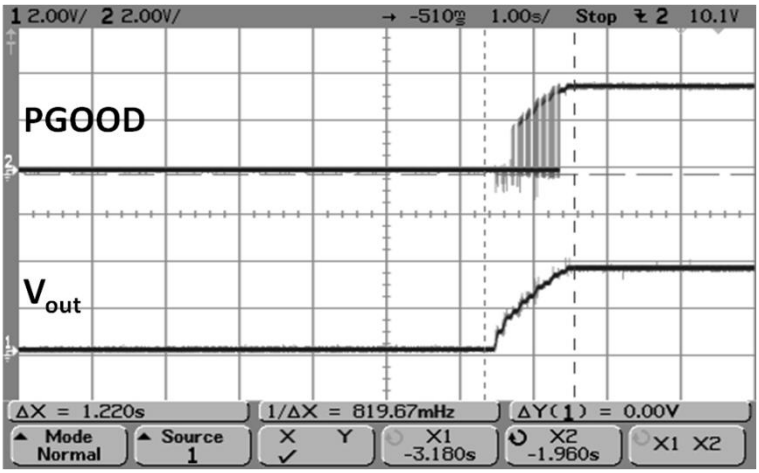

Figure 4.6 - Test with a 76µA load and 2200µF capacitor.

Besides the piezoelectric generator another generator was also studied –the Magnetic Switch. All the results for these tests performed with both generators are all organized in Tab.7, 8 and 9 in the next section.

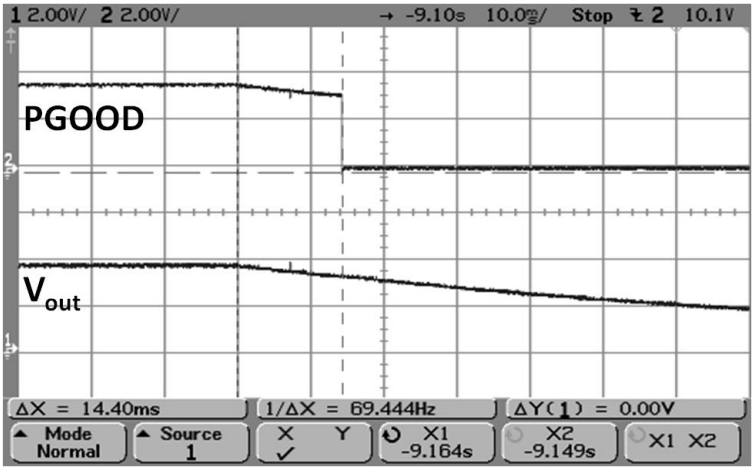

Figure 4.7 – Test with a 90mA load and 2200µF capacitor.

4.3.3 - Analysis

In a general way, it is possible to see that the LTC5388 was operational and working as expected. Moreover, since the chip has a 20V limit the piezoelectric generator is generating power with enough magnitude.

In order to draw some conclusions about the testing frequency environment the resulting frequency measurement done in the second experiment is compared to values found in literature. According to [28], which reports the results from a device build to measure the arm motion frequency, a 0,75Hz arm motion frequency is considered as “very high rate”. So, since to induce displacement to the transducer no electric equipment such as a vibrational platform or a shaker is used, the frequency is not constant, but according to measurements the operation frequency value is way up the value found in literature. On the other hand, when analyzing the piezoelectric signal it is noticeble that energy does not reach as high negative voltage difference as the almost positive 20 V. This is due to the fact the manually vibration induces a displacement in one way only and this way the piezo instead of vibrating is only shrinking and returning to the the natural posititon, like a string that is compressed but not streched. Therefore, the piezo generator is not being properly stimulated with consequences on the power generatation. With a proper vibration source the piezoelectric device would generate twice the power. With a first view toward the remaining test’s results it is clear the highly marked difference between the two load values. This difference is specially noticed in the discharging time values since it decreases dramatically with the higher load on both generators. On the other hand, these values rise when using a bigger output reservoir. This means that despite being capable of handling the load for more time, the capacitor also takes a longer time to charge. What stands out the most between the two generators is the difference between charging and discharging times. As it can be seen the magnetic switch discharge time is lower however, unlike the piezoelectric generator this device charged the 2200 µF capacitor by itself without using a power source.

Table 4.4 - Piezoelectric generator results with a 70 µA load.

	no vibration	vibration	no vibration	vibration
C_{out}	47 µF	47 µF	2200 µF	2200 µF
I_{load}	70 µA	70 µA	70 µA	70 µA
t_{charge}	-----	20 ms	----	1,2s
$t_{discharge}$	204ms	-----	8s	-----

Table 4.5 - Piezoelectric generator results with a 92mA load.

	no vibration	vibration	no vibration	vibration
C_{out}	47 µF	47 µF	2200 µF	2200 µF
I_{load}	92 mA	92 mA	92 mA	92 mA
t_{charge}	----	It does not charge	----	It does not charge
$t_{discharge}$	3,2 ms	3.6 ms	14.4 ms	24.0 ms

This factor is probably responsible for the time differences. With the power source the output capacitor reaches its maximum capacity. These results not only show us the power system capability but do also present a clear relationship between this and the frequency availability. The different values for both vibration environments show how the system is dependent of the frequency. It is noticed especially in the Sleep MODE tests where the system with continuous vibration can handle the load indefinably but with no vibration the system only lasts for 204ms.

Table 4.6 - Magnetic switch generator results with a 70µA load.

	Magnetic Switch	
C_{out}	47 µF	2200 µF
I_{load}	70 µA	70 µA
t_{charge}	780 ms	28 s
$t_{discharge}$	144 ms	14.2 s

4.4 - Alternative Studies

Besides the tests with the piezoelectric another approach is studied as well, harvesting thermal energy. Therefore, in order to know the viability of integrating also a thermic generator in the device power system the efficiency was first studied. To estimate this value it is assumed that the body temperature- T_{body}- is T_{high} and the environmental temperature - $T_{environment}$ – is T_{low} and according to the expression 3.1 the Carnot Efficiency is calculated as follows. For the enviornment temperaturature, three different scenarios are considered. The scenarios correspoding to Summer and Winter are based in the respective season average temperature. Moreover, since the device end is to be used by swimmers it follows natural to consider a swimming pool water temperature.

The results are summarized in Tab.10. It is noticeable the resulting low effciency values.

Table 4.7 - Thermal energy efficiency.

	T_{body}	$T_{environment}$	**Carnot Efficiency**
Pool Water	310 K	301 K	3 %
Winter	310 K	290 K	6.4 %
Summer	310 K	276 K	12.3 %

4.5 - Conclusions

The results are very enlightening about the effectiveness of a potencial use of a powering system such as this. It is noticeble the low capacity for the system to support a load for long periods of time, particullary in active mode where it can only handle the load for a few miliseconds, not enough for the 20ms needed to do a transmission. Therefore, the presented system configuration can not feed a load in a continuous mode and therefore it will not be capable to power the portable device as well. However, this system might be usefull to power other applications such as wi-fi sensor nodes. These systems also operate in discontinuoues mode since they consume energy taking a sample and after consume energy again to send it to a remote computer. The main difference is its low duty cicle and power needs. The time in between sleep and active is enough to harvest energy to the next operation while the time that is active is small enough to be powered by the stored energy. Fig.4.8 shows the power generated and the power consumed respectively of ideal discontinuos system where the average power generated is higher than the power consumed. Moreover, a typical sensor node consumption is between 5 and 10 μW [29]. The consumption values are significantly below the project power budget values. This means that the tested system can support these amounts of load if placed in a proper continuous vibration energy source.

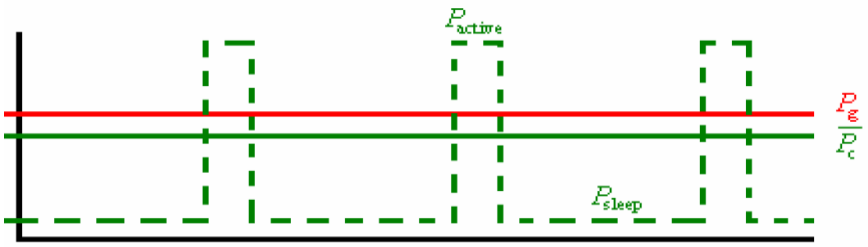

Figure 4.8 – Pg > Pc [14].

Finally, a standalone piezoelectric power generator system cannot provide enough power to devices with power needs above 250 μW and 360mW and duty cycles of a dozen of seconds and milliseconds for sleep and active mode respectively.

Chapter 5

Final System

5.1 - Introduction

Since the initial power system did not achieved the expected results some changes have had to be done in order to increase the power system performance. As it shown in Fig.5.1 the main change was switching the LTC3588-1 storage unit from the output to the input and instead of a regular capacitor, a 1 F supercapacitor was used. Besides these hardware modifications, another important part of the research is also integrated, the low power efficiency regarding the ATMEL microcontroller software. The performed changes and the obtained results are described in the present chapter.

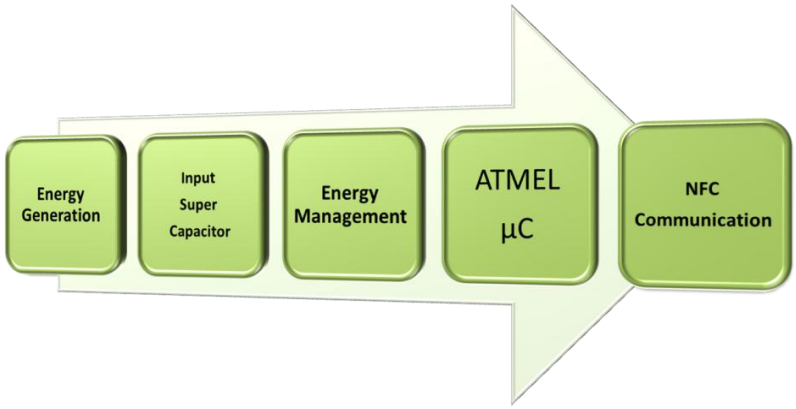

Figure 5.1 – Final system block diagram.

5.2 - Microcontroller ATMEL ATMEGA1284P

This microntroller operation aims size-constrained and low-power applications..Due to its technology, known as *picoPowe,r* it can consume current down to 1µA. This level of

consumption can be achieved using an ATMEGA1284P feature, the sleep modes. These modes make the microcontroller enter in a state where the main clock is disabled as well as other units that can be selected by the user.

5.3 - Software Development

Before designing the software a carefully annalysis to sleep modes consumption and operation is performed, the measurements are present in Tab.5.1. The Power Down Mode along with the Power Save mode are the modes that consume less power however, there are some major differences between them. While the Power Down disables all clock sources and can only be awake by an external interruption the Power Save mode leaves a timer running, if configured correctly the timer can awake the device. On the other hand the Power Save mode will only work at 1.1µA if an external oscillator is used to coordinate the timer. In this project the microcontroller internal clock is used. Considering these two power modes, the one that best fits to the project is the Power Save Mode since it allows being awakened in a regular time basis. Moreover, it is also important to refer that if the clock is previously prescaled it will reduce the power consumption significantly.

Table 5.1 –Consumption measurements of the different ATMEL1284P sleep modes.

Mode	Prescaled Clock	Timer1	Timer2	Timer2 TOSC	Consumption
Active					1.75mA
Active	✓				1.08mA
Active		✓			1.82mA
Idle					1.028m
Idle	✓				947 µA
Save			✓		163.3µA
Save				✓	1.1µA
Save	✓		✓		110.1µA
Down					1µA

To programming C language is used as well as AVR Studio 4 load the program into the micro controller using a JTAG interface. After the overview throughout the sleep modes the program was designed resulting on the block diagram present in Fig.5.2. The programm consists in six different states: SLEEP, WakeUP, RFON, ACTIVE, BATCHECK and LBAT. The first two states are the low power core of the system since it is where the software waits for a request to perform an action.

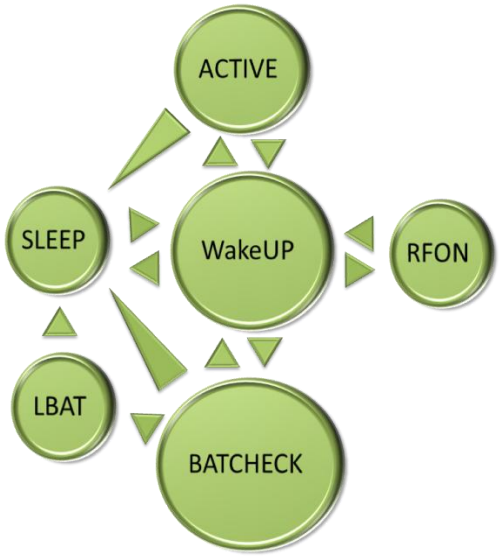

Figure 5.2 - Software block diagram.

The SLEEP state corresponds to Power Save mode while the WakeUP state is where the programm checks if some action was requested by the user. These actions are two and correspond to states: ACTIVE and RFON. The ACTIVE mode enables the user to manually wake up microcontroller while the RFON allows to simulate an NFC transmission. These two modes are connected by hardware to two pression buttons. The remainning modules correspond to a regular battery check performed by the system in the BATCHECK block and if the battery is low the proper measures are performed in LBAT otherwise the micro will enter the sleep state again. After programming the microntroller some more consumption measurements we're performed. This time direccioned to know how much power each state consumes. These values are shown in Tab.5.2. Given this, it is possible to define the parameters corresponding to an NFC transmission: this operation consumes 90mA during 20ms.

Table 5.2 – Consumption of each software state.

	Sleep/WakeUP	Active	Active (Idle Mode)	RFON
Consumption	224µA	1,9mA	1,15	90mA

5.7 - Hardware Development

To test the software a printed circuit board was designed and built, Fig.5.3. The board includes the ATMEL 1284P a JTAG interface and also a communication pad to the NFC communication interface chip, the PN532.

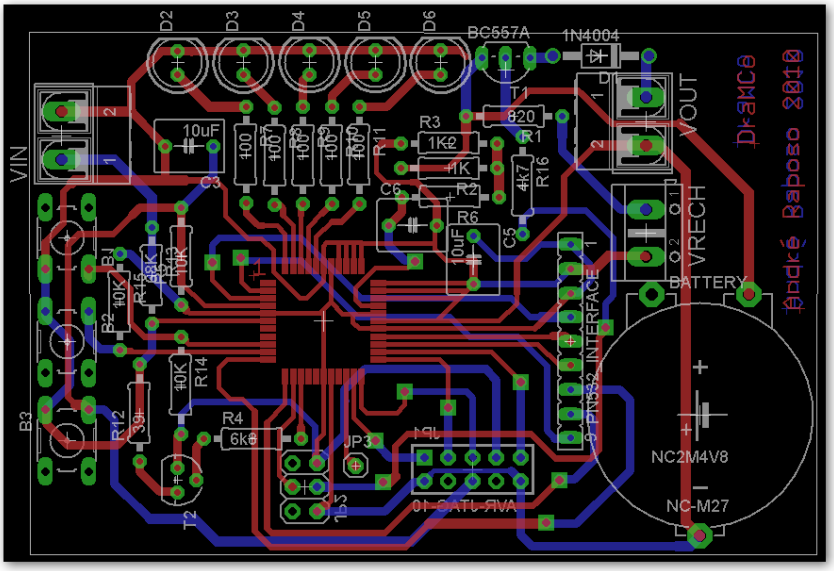

Figure 5.3 - Final board design

Besides these main units three buttons and five LEDs are also embedded. One of the buttons is the RESET button while the other two are responsible for the manual awake and the NFC transmission simulation. This simulation is performed by a switch and two different loads connected to it. In the Fig.5.4 it is visible both Active and Sleep loads connected to both ends of the switch. The state of the switch is controlled by software trough the signal LOAD defined as an output. Moreover, the board was designed to be used not only with the energy harvest supply but also with a battery and a recharge module which is plugged to the VRECH connector. The VOUT connector is meant to be connected between the V_{in} pin of the LTC33588-1 and the ground while the VIN input objective is to receive the energy provided by energy harvest power supply.

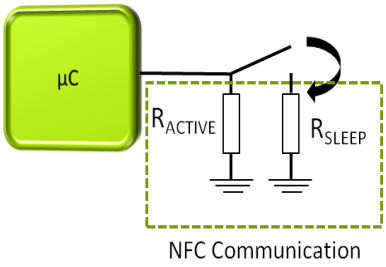

Figure 5.4 - NFC transmission simulation procedure.

5.5 - Tests

At this stage the final system was properly connected, programmed and ready to be tested. On these tests, a power source regulated to match the same amplitude and frequency showed in Fig.4.5 is used instead of directly using the piezoelectric structure. Moreover, an ammeter is connected to verify if the microcontroller is operating and to check if it operating in the correct state.

First, the power source was turned on until V_{out} reached the regulation point and turned off after. After this point the microcontroller was operating at 220 μA and the system was holding up easily with no changes in the V_{out} and PGOOD curves observed in the oscilloscope. After checking the SLEEP mode, the press button responsible to switch to ACTIVE mode was pressed and the controller started to consume the expected 1,9mA also with no trouble since the PGOOD remained high during all this time. Finally, the RF ON transmission was simulated and this time the output drop down but on the other hand it took only a few seconds to the system recover again with vibration energy presence. Since the system's response wasn't very effective regarding the RF transmission, this time the power source charged the capacitor for five minutes. This way the system response improved, and it could handle at least two NFC transmissions.

Until this point, the system has responded well to these tests therefore, other tests must be realized to know exactly the capabilities of the power system. Given this, it was defined a time interval of an hour as shown in Fig.5.5 where the device will operate without vibration energy input. During this hour a RF ON load is applied and one battery check runs one time per minute, the remaining time the system is in SLEEP mode. This way it is possible to have a clear idea about the device autonomy. Before running the test the vibration source is turned on during ten minutes. After this procedure, the system carried these loads during approximately three hours until the V_{out} drop down below the selected output voltage after a transmission simulation. After the system was down the power source was turned on again. It took around five minutes to the rise PGOOD signal high. From this point the system was ready again to power the device following the load diagram, (Fig.5.5) for at least one hour more.

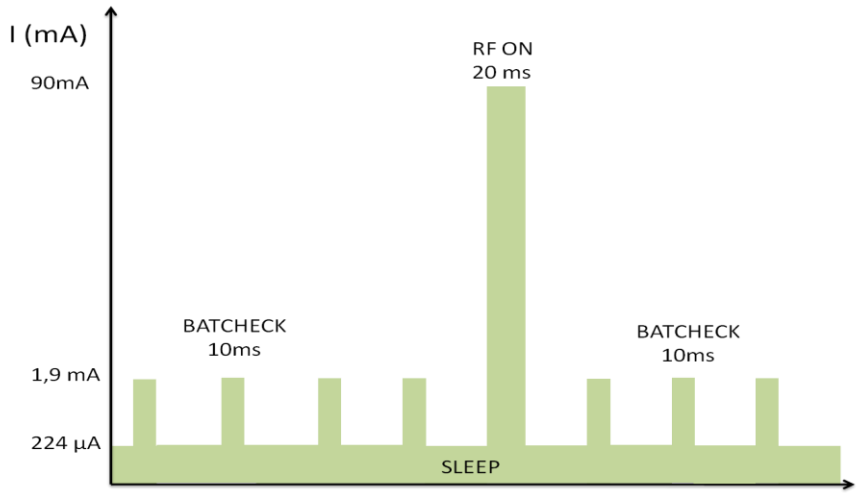

Figure 5.5 - Test diagram.

5.6 - Analysis

It is evident the dramatically increase of effectiveness of the power system in the last test results. Not only the discharge times increased but the system is now also not as dependent of vibration energy as it was in the first configuration. Even without a presence of vibration it can power the microcontroller and the NFC communication interface for a few hours. Still, some difficulties are noticeable handling the higher loads, since it can only handle four communications in four hours, which means one communication per hour. In a real life scenario this use rate can be higher. Although this system is not perfect to work by its own, it can very usefull if used to enhance a battery life. Therefore, to have a precise notion of how much this system can improve a system's autonomy let's consider a system using only a battery and the same energy loads defined in the previous section showed in Fig.5.5. However, this time three transmissions will occur in one hour instead of one. To calculate the energtic weight of each state this expression was used,

$$I_{TOTAL} = I_{STATE}.t_{STATE}.n\,(\text{mAh}) \tag{5.1}$$

Where I_{STATE} represents the current consumed by the state, t_{STATE} the time each state lasts and *n* the number of times that each load is used in one hour. The obtained results are present in Tab.5.3.

Table 5.3 - Total load of each state.

	RF ON	ACTIVE	SLEEP	Total	Units
I_{TOTAL}	1.5	0.633	**0.062**	2.195	µAh

Despite not handling very well the high loads, the power system could power the device in sleep and active mode for several hours with no vibration, which means that if a vibration source is periodically present the SLEEP and ACTIVE modes can be handled indefinently. Given this, the energy burdens can be distributed by the piezo system as well and this way the amount of energy carried by the battery would be smaller as shown in Fig.5.6. If the battery is only in charge of the higher load then the amount of energy would be reduced to 1.5 µAh which means it would save a lot of battery energy. Comparing to the first assumption where only the battery is used, using the piezo electric generator it can save 66,45% of the battery power which would highly increase the battery lifetime substantially.

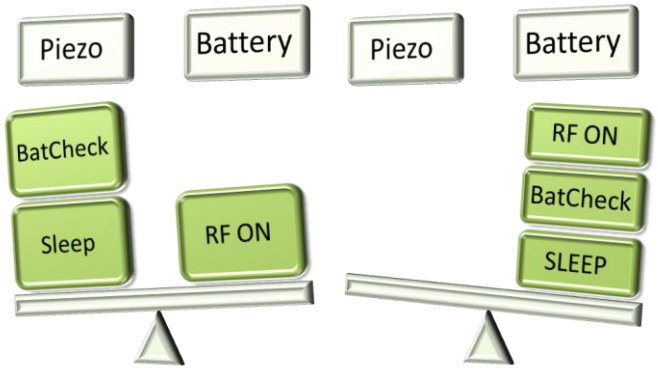

Figure 5.6 – Energy burdens distribution.

5.7 - Conclusion

The performed changes had a big impact on the response of the system. Configured this way, the system can now be classified as a viable solution to power low consumption electronic devices or even to work together with a battery in order to improve its lifetime. Moreover, if the user's wrist can provide enough vibration energy to keep charging the system will be even more effective and save even more battery power.

Chapter 6

Conclusion

During the project developed at DraMCO research group a power system based on a new technology – Energy Harvesting - was studied and tested. The power system uses vibration energy together with an energy management system constituted by a Linear Technology microchip – LTC3588-1. The objective is to power a Near Field Communication interface device.

In the first stage of the present research the accomplished results were unsatisfatory. The system was highly frequency dependent and the power deliver rate was very low. Configured this way the system could handle loads around a few μA only during a dozen of ms. After the described changes the system effectiveness increased drammatically and results achieved the main objectives. The final system is working according to what was initially specified since it can feed a microcontroller and an Near Field Communication interface using Energy Harvesting technology. Given this, energy harvesting is a feasible solution to power low consumption devices. With future developments such as increasing the storing capacity it can become a viable alternative to the use of batteries, especially if used in places where the environmental energy is abundant.

Still, the system has space for further improvements. An external clock can be used to diminish the ATMEl power consumption together with a higher autonomy battery. In adittion, using fabrication processes techniques such as CMOS or MEMS the system can be embedded in a small system and this way integrated in a portable device.

Another topic approached was the NFC communication protocol. This technology takes advantage of RFID operation to create a two-way communication solution with a wide range of applications, especcialy when integrated in portable comunication devices.

References

[1] Ecma International: Standard ECMA – 340, Near Field Communication Interface and Protocol (NFCIP-1), December 2004.

[2] Ecma International: Standard ECMA – 352, Near Field Communication Interface and Protocol -2 (NFCIP-2), December 2003.

[3] M.Ferrari, V.Ferrari, M.Guizzetti, D.Marioli, A.Taroni, "Piezoelectric multifrequency energy converter for power harvesting in autonomous microsystems". Sensors and Actuators A: Physical, Volume 142, Issue 1, 10 March 2008, Pages 329-335.

[4] Jing-QuanLiu, Hua-BinFang, Zheng-YiXu, Xin-HuiMao, Xiu-ChengShen, DiChen, Hang Lião, Bing-Chu Cai, "A MEMS-based piezoelectric power generator array for vibration energy harvesting", Microelectronics Journal, Volume 39, Issue 5, May 2008, Pages 802-806.

[5] M.Ferrari, V.Ferrari, M. Guizzetti, B.Andò, S. Baglio, C. Trigona, "Improved Energy Harvesting from Wideband Vibrations by Nonlinear Piezoelectric Converters", Procedia Chemistry, Volume 1, Issue 1, September 2009, Pages 1203-1206.

[6] I.Sari, T.Balkan, H.Kulah, "An electromagnetic micro power generator for wideband environmental vibrations", Sensors and Actuators A: Physical, Volumes 145-146, July-August 2008, Pages 405-413.

[7] P.Glynne-Jones, S.P.Beeby, N.M. White, "Towards a piezoelectric vibration-powered microgenerator", IEE Proc. Sci., Meas. Technol., vol. 148, 2001, Pages 69-72.

[8] L.Mateu, F.Moll, "Review of Energy Harvesting Technique and Applications for Microelectronics", Proc. SPIE, Vol. 5837, 359 (2005), doi:10.1117/12.613046.

[9] S.P. Beeby, M.J.Tudor, N.M. White, "Energy Harvesting vibration sources for microsystems applications", Measurement Science and Technology, 17 (12), 2006. R175-R195.

[10] Eli S.Leland, Jessy Baker, Eric Carleton, Elizabeth Reilly, Elaine Lai, Brian Otis, Jan M.Rabaey, Paul K.Wright, "Improving Power Output for Vibration-Based Energy Scavengers", IEEE Pervasive Computing. 2005.

[11] Y.Zhu, S.O.R. Moheimani, M.R. Yuce, "A 2-DOF Wideband Electrostatic Transducer for Energy Harvesting and Implantable Applications" in IEEE Conference on Sensors (IEEE SENSORS 2009), Pages 1542-1545, October 2009.

[12] Gou-Jen Wang, Wen-ChunYu, Ying-HsuLin, Hsiharng Yang, "Modeling and fabrication of a piezoelectric vibration induced micro power generator" in Journal of the Chinese Institute of Engineers, Vol. 29, No. 4, Pages 697-706, 2006.

[13] Adilson J.Cardoso, Cesar R.Rodrigues, Rafael S.Pippi, Cesar A.Priorand Filipe C.B. Vieira, "CMOS Energy Harvester Based on a Low-Cost Piezoelectric Acoustic Transducer" in Proc. of the 49th IEEE International Midwest Symposium, Vol.1, Pages 70-74, 2006.

[14] M.T.Penella, M.Gasulla, “A Review of Commercial Energy Harvesters for Autonomous Sensors” in Instrumentation and Measurement Technology, Conference – IMTC 2007 Warsaw, Poland, May 1-3, 2007.
[15] Satoru Fujishima, “The History of Ceramic Filters” , IEEE transactions on ultrasonics, ferroelectrics, and frequency control, vol. 47, no. 1, January 2000.
[16] Dongna Shen, Jung-Hyun Park, Joo Hyon Noh, Song-Yul Choe, Seung-Hyun Kim, Howard C.Wikle III, Dong-Joo Kim, “Micromachined PZT cantilever based on SOI structure for low frequency vibration energy harvesting”, Sensors and Actuators A: Physical, Volume 154, Issue 1, 31 August 2009, Pages 103-108.
[17] R.J.M. Vullers, R. van Schaijk, I.Doms, C. Van Hoof, R. Mertens, “Micropower energy harvesting”, Solid-State Electronics, Volume 53, Issue 7, July 2009, Pages 684-693.
[18] Loy Chuan Chia, Bo Feng, “The development of a micropower (micro-thermophotovoltaic) device”, Journal of Power Sources, Vol.165, Pages 455-480, January 2007.
[19] G.Jeffrey Snyder, “Small Thermoelectric Generators”, Interface, 2008, Pages 54-56.
[20] Darren McCarthy, “Evaluating and optimizing RFID and NFC systems using real-time Spectrum analysis”, April 2006, Pages 32-38.
[21] Thad Starner, Joseph A.Paradiso, “Human Generated Power for Mobile Electronics”, Low-Power Electronics, CRC Press, Chapter 45, 2004, Pages 45-1 - 45-35.
[22] Paul Wright, “Energy Scavenging/Harvesting”, Center for Information Technology Research on the interest of Society, March 8th 2006.
[23] Kompis Costis, Aliwell Simon, “Energy Harvesting Technologies to Enable Remote and Wireless Sensing”, June 2008.
[24] Whitaker Michael, “Energy Harvester Produces Power from Local Environment, Eliminating Batteries in Wireless Sensors”, LT Journal of Analog Innovation, Vol. 20 , April 2010.
[25] http://cds.linear.com/docs/Datasheet/35881f.pdf, Access in March 2010.
[26] Adptative Energy, “Building Blocks of an Energy Harvesting Solution”, July 2009.
[27] O’Neil Bob, Mitchell Brad, Ludlow Chris, “First Draft of Standard on Vibration Energy Harvesting”, 2nd Annual Energy Harvesting Workshop, January 30 – 31, 2007.
[28] Bernmark, Eva, Wiktorin, Christina, “A triaxial accelerometer for measuring arm movements”, Applied Ergonomics, Volume 33, Issue 6, November 2002, Pages 541-547
[29] Seeman Michael, Seth Sanders, “Harvesting Micro-Energy”, University of California, February 2009.
[30] http://www.nfc-forum.org/specs/, Access in March 2010.